


# ALS-Associated KIF5A Mutation Causes Locomotor Deficits Associated with Cytoplasmic Inclusions, Alterations of Neuromuscular Junctions, and Motor Neuron Loss

Laurent Soustelle, Franck Aimond, Cristina López-Andrés, Véronique Brugioti, Cédric Raoul, and  Sophie Layalle

Institute for Neurosciences Montpellier, Université Montpellier, Institut National de la Santé et de la Recherche Médicale, Montpellier, 34091, France

Amyotrophic lateral sclerosis (ALS) is a fatal neurodegenerative disease affecting motor neurons. Recently, genome-wide association studies identified KIF5A as a new ALS-causing gene. KIF5A encodes a protein of the kinesin-1 family, allowing the anterograde transport of cargos along the microtubule rails in neurons. In ALS patients, mutations in the KIF5A gene induce exon 27 skipping, resulting in a mutated protein with a new C-terminal region (KIF5A  $\Delta$ 27). To understand how KIF5A  $\Delta$ 27 underpins the disease, we developed an ALS-associated KIF5A *Drosophila* model. When selectively expressed in motor neurons, KIF5A  $\Delta$ 27 alters larval locomotion as well as morphology and synaptic transmission at neuromuscular junctions in both males and females. We show that the distribution of mitochondria and synaptic vesicles is profoundly disturbed by KIF5A  $\Delta$ 27 expression. That is consistent with the numerous KIF5A  $\Delta$ 27-containing inclusions observed in motor neuron soma and axons. Moreover, KIF5A  $\Delta$ 27 expression leads to motor neuron death and reduces life expectancy. Our *in vivo* model reveals that a toxic gain of function underlies the pathogenicity of ALS-linked KIF5A mutant.

**Key words:** amyotrophic lateral sclerosis; axonal pathology; *Drosophila*; Kinesin

## Significance Statement

Understanding how a mutation identified in patients with amyotrophic lateral sclerosis (ALS) causes the disease and the loss of motor neurons is crucial to fight against this disease. To this end, we have created a *Drosophila* model based on the motor neuron expression of the KIF5A mutant gene, recently identified in ALS patients. KIF5A encodes a kinesin that allows the anterograde transport of cargos. This model recapitulates the main features of ALS, including alterations of locomotion, synaptic neurotransmission, and morphology at neuromuscular junctions, as well as motor neuron death. KIF5A mutant is found in cytoplasmic inclusions, and its pathogenicity is because of a toxic gain of function.

## Introduction

Amyotrophic lateral sclerosis (ALS) is a fatal neurodegenerative disorder characterized by the selective and progressive loss of motor neurons (Cleveland and Rothstein, 2001). Clinical signs begin with muscle weakness, which progresses over time to fatal respiratory failure; ~90% of ALS cases are sporadic, with the remaining cases predominantly associated with a dominant inheritance pattern. To

date, >30 genes have been identified as being causative of the disease; of these, *C9orf72*, *SOD1*, *TARDBP*, and *FUS* account for ~60% of the genetic cases in Europe (Gregory et al., 2020). Recently, two studies using either whole-exome sequencing or genome-wide association studies have identified *KIF5A* as a new gene associated with ALS (Brenner et al., 2018; Nicolas et al., 2018).

KIF5A belongs to a family of motor proteins, called kinesin. Kinesins form a large superfamily to date of 45 genes (*KIFs*), grouped into 14 different families in vertebrates (Miki et al., 2001; Hirokawa and Takemura, 2005). These proteins are microtubule-bound and orchestrate intracellular transport, generally toward the plus end of microtubules (Hunter and Allingham, 2020). In neurons, kinesins are the main motor proteins that, in axons or dendrites, contribute to active anterograde transport of different cargos, such as protein complexes, mRNAs, or organelles (Guillaud et al., 2020).

The kinesin-1 family consists of three members: KIF5A and KIF5C are specifically expressed in neurons and KIF5B is ubiquitously expressed (Kanai et al., 2000; Miki et al., 2001). Kinesin-1

Received Mar. 28, 2023; revised Sep. 12, 2023; accepted Sep. 13, 2023.

Author contributions: L.S., C.R., and S.L. designed research; L.S., F.A., C.L.A., V.B., and S.L. performed research; L.S. and S.L. analyzed data; L.S., C.R., and S.L. wrote the paper.

This work was supported by Institut National de la Santé et de la Recherche Médicale and Association pour la Recherche sur la Sclérose Latérale Amyotrophique Grant R19101FF. We thank the Bloomington Stock Center, the Developmental Hybridoma Bank for providing fly lines and antibodies and the Montpellier MRI imaging platform; and all members of the laboratory for discussion and support.

The authors declare no competing financial interests.

Correspondence should be addressed to Laurent Soustelle at laurent.soustelle@inserm.fr or Sophie Layalle at sophie.layalle@inserm.fr.

<https://doi.org/10.1523/JNEUROSCI.0562-23.2023>

Copyright © 2023 the authors

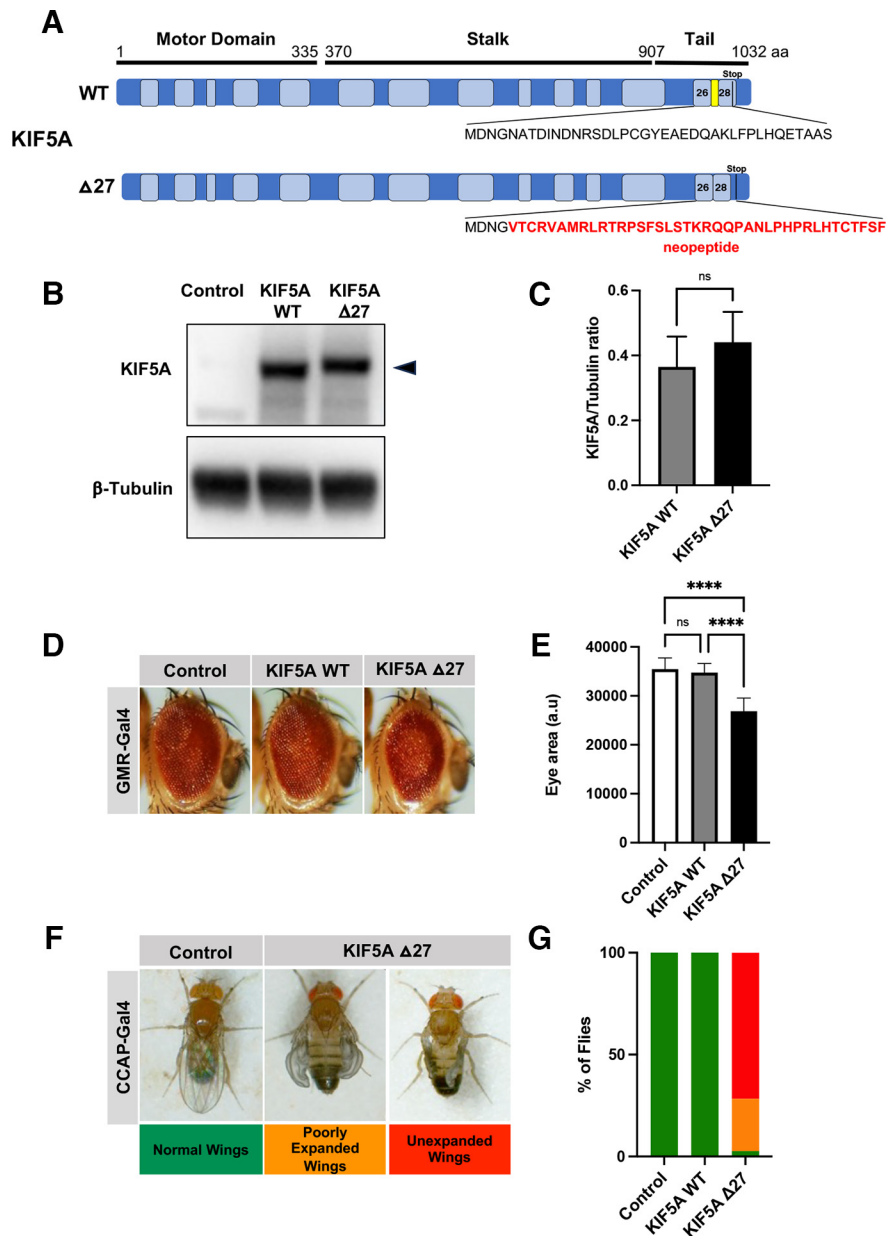


**Figure 1.** The human ALS-causing mutation KIF5A  $\Delta$ 27 is pathogenic in *Drosophila* neurons. **A**, Blue and light blue represent the 29 exons of KIF5A. The different domains of the kinesin are indicated. In the KIF5A WT protein, the translation stop codon is localized in exon 28 (dark line). The mutations found in ALS patients affect the splicing of exon 27 (yellow exon), leading to its nonincorporation in the mutant protein (called KIF5A  $\Delta$ 27). The skipping of exon 27 induces a translational frameshift, which leads to a new C-terminal region in the  $\Delta$ 27 mutant protein. Red represents the resulting 39 amino acid neopeptide. **B**, **C**, Western blot analysis of KIF5A expression and quantification. Total protein extraction was performed from heads of control (GMR-Gal4/+), KIF5A WT (GMR-Gal4/UAS-KIF5A WT), and KIF5A  $\Delta$ 27 (GMR-Gal4/UAS-KIF5A  $\Delta$ 27) expressing flies. Top, Anti-KIF5A staining (black arrowhead). Bottom, Anti- $\beta$ -tubulin, used as a loading control. Quantification of gel bands was done by using Fiji software (Analyze gels); five gels were analyzed. Data are mean  $\pm$  SD. Mann-Whitney test was used to assess statistical significance. **D**, Five-day-old adult flies expressing either KIF5A WT or  $\Delta$ 27 in eyes under the control of the GMR-Gal4 driver at 28°C. **E**, Eye area is quantified for each genotype. a.u., Arbitrary units. Flies expressing KIF5A  $\Delta$ 27 display a severe reduction of eye size, while KIF5A WT has no effect compared with control flies ( $n = 10$  flies for each genotype). Data are mean  $\pm$  SD. ns,  $p > 0.05$ , \*\*\*\* $p < 0.0001$ ; one-way ANOVA test with Tukey *post hoc* test. **F**, Representative flies showing control with normal wings as well as poorly expanded or unexpanded wings when KIF5A  $\Delta$ 27 is expressed in CCAP neurons. **G**, Percentage of flies with normal (green), poorly expanded (orange), or unexpanded (red) wings. Expression of KIF5A  $\Delta$ 27 produced 71.7% and 25.7% of flies with unexpanded and poorly expanded wings, respectively, as well as 2.6% of flies with normal wings. In comparison, all control and KIF5A WT-expressing flies had normal wings.  $n = 140$ , 123, and 113 for the control, KIF5A WT, and KIF5A  $\Delta$ 27 condition, respectively.

forms a dimeric heavy chain structure (KHC) to move along microtubules. KHC is composed of three main domains (see Fig. 1A): the N-terminal part is the motor domain (also called the head domain), which contains the microtubule and ATP-binding sites; the C-terminal of the protein is the tail domain that mediates binding to different cargos. These domains are connected by the central stalk domain responsible for the dimerization of two KHC monomers (Qin et al., 2020; Cason and Holzbaur, 2022).

In the C-terminal part, KHC dimers form a complex with a dimer of Kinesin light chain proteins (Brady, 1985; Vale et al., 1985; Hirokawa et al., 1989). Kinesins are known to transport multiple cargos into axons by binding to distinct adaptor proteins that ensure the specificity of the kinesin-cargo interactions.

The global genetic ablation of *Kif5a* gene in mice is lethal early after birth (Xia et al., 2003); however, the conditional *Kif5a* deletion leads to seizures and death within 3 weeks for most

animals, likely because of alteration of GABA<sub>A</sub> receptor trafficking (Xia et al., 2003; Nakajima et al., 2012).

Primary motor neuron cultures from *Kif5a* KO mice showed decreased survival and reduced axonal and dendritic outgrowth (Karle et al., 2012). In addition, alteration of mitochondrial transport was observed in the axons of *Kif5a* mutant motor neurons (Karle et al., 2012). Similar results have been obtained in zebrafish where the loss of *kif5a* generates a defect in the axonal transport of mitochondria and degeneration of peripheral neuron axons (Campbell et al., 2014).

Most ALS-associated KIF5A mutations affect the C-terminal part of the kinesin, particularly the splicing sites of exon 27, resulting in its skipping and the formation of a KIF5A protein with a neo-formed C-terminal part (Brenner et al., 2018; Nicolas et al., 2018) (see Fig. 1A). Interestingly, mutations in KIF5A linked to other neurodegenerative diseases have already been identified. These mutations affect the N-terminal of the KHC protein and lead to hereditary spastic paraplegia Type 10 (SPG10) (Reid et al., 2002; Kawaguchi, 2013; Qiu et al., 2018), Charcot-Marie-Tooth type 2 (CMT2) (Fichera et al., 2004; Blair et al., 2006; Crimella et al., 2012), or distal spinal muscular atrophy (de Fuenmayor-Fernández de la Hoz et al., 2019). Frameshift mutations at the C-terminal of KIF5A have also been reported in cases of patients suffering from neonatal-intractable-myoclonus (Duis et al., 2016; Rydzanicz et al., 2017). Recently, studies have investigated the effects of the ALS-related mutant form of KIF5A (KIF5A  $\Delta$ 27) in neurons derived from ALS patients induced pluripotent stem cells (Baron et al., 2022; Nakano et al., 2022; Pant et al., 2022). *In vitro* assays showed that the motor activity of KIF5A  $\Delta$ 27 protein is not impaired and that its processivity is increased compared with KIF5A WT. The authors showed that KIF5A  $\Delta$ 27 can form cytoplasmic inclusions that are associated with an increased rate of cell death and a toxic gain of function (Nakano et al., 2022; Pant et al., 2022). To explore the pathogenic mechanisms of KIF5A  $\Delta$ 27 in a physiological context, and integrated *in vivo* system, we used *Drosophila* as a model.

Here, we show that KIF5A  $\Delta$ 27 expression in motor neurons induces a locomotor behavioral defect characterized by posterior paralysis, which is the hallmark of axonal physiological defects. Indeed, we show that both the morphology and synaptic transmission at the neuromuscular junction (NMJ) level are notably altered. Cytoplasmic inclusions of KIF5A  $\Delta$ 27 are found in the soma and axons of motor neurons. *In vivo*, expression of KIF5A  $\Delta$ 27 is neurotoxic toward motor neurons and induces larval death when expression is reinforced. Overall, our results describe a *Drosophila* model that recapitulates the main features of ALS and demonstrate that KIF5A  $\Delta$ 27 acts via a toxic gain of function to lead to motor deficits.

## Materials and Methods

**Fly strains.** All *Drosophila* stocks were raised on standard cornmeal medium under temperature-controlled conditions and crosses were performed at 25°C, unless otherwise mentioned. Experiments were performed on both male and female excepted when mentioned.

The *Drosophila* strains VGlut-Gal4 (OK371-Gal4, #26160), CCAP-Gal4 (#25685), GMR-Gal4 (#8605), UAS Mito-GFP (#8443), UAS-GFP (#32201), and tub-Gal80<sup>ts</sup> (#7017) were obtained from the Bloomington Stock Center. UAS NPY-GFP was obtained from I. Robinson (Cambridge, UK). Control condition for each experiment was done by the cross of the driver Gal4 line with the *w*<sup>CantonS</sup> line used as WT stock.

The larval lethality experiment was conducted at 29°C. After allowing the different crosses to lay for 24 h, early L1 larvae were collected in a

fresh tube, with 50 larvae per tube. The number of pupae formed was then counted for each genotype.

Stocks used for the longevity assay were backcrossed into a *w*<sup>CantonS</sup> (the line used as WT) background for six generations.

For the UAS-KIF5A transgenic lines, full-length cDNAs of the WT and  $\Delta$ 27 mutant human KIF5A were synthesized (Gene Universal) and cloned into a pcDNA3.1(+) plasmid. The cDNAs were then subcloned into a pUAST and random transgenesis was performed by BestGene. From the transgenic lines obtained, some were selected to ensure a similar level of protein expression between the WT and  $\Delta$ 27 mutant by using the GMR-Gal4 driver.

**Larval locomotion.** The protocol has already been described by Devambaz et al. (2017). Briefly, third instar larvae were placed at the center of a Petri dish filled with grape juice agar. Larval locomotion was video-recorded for 2 min with a camera (Sony HDR-CX240), and movies were analyzed with the Fiji plugin manual tracking.

**Western blot.** Protein extracts were prepared from the heads of *Drosophila* expressing KIF5A under the control of the GMR-Gal4 driver, dissected larval CNSs, or adult thoraxes of VGlut-Gal4/UAS-KIF5A animals. Cell homogenization and lysis were done in RIPA buffer (150 mM sodium chloride, 1% NP-40, 0.5% sodium deoxycholate, 0.1% SDS, 50 mM Tris, pH 8.0, supplemented with protease inhibitor cocktail from Roche Life Science) for 2 h at room temperature. Then, Laemmli buffer was added and the samples were boiled for 5 min. Samples were analyzed by SDS-PAGE using Mini-PROTEAN TGX precast gels (Bio-Rad). Separated proteins were transferred onto nitrocellulose membranes using Trans-Blot Turbo (Bio-Rad). Primary and secondary antibodies were incubated in 5% milk in PTX (PBS, 0.1% Triton X-100), and washes were done with PTX. Immunodetection was done with Clarity Western ECL kit (Bio-Rad). Chemiluminescence detection was acquired with Fusion Fx system (VILBER). The following primary antibodies were used: mouse anti-KIF5A (1/1000, Santa Cruz Biotechnology sc-376452), mouse E7 (1/400, anti- $\beta$  tubulin from DSHB). Secondary antibody used was HRP-linked goat anti-mouse (1/10,000, Jackson ImmunoResearch Laboratories).

**Immunostaining.** Wandering third instar larvae were dissected in fillets in PBS, 1 mM EDTA and fixed in 4% EM-grade PFA (Fisher Scientific) in PBS for 20 min at room temperature. Primary antibodies were incubated in PBS 0.3% Triton, 1% BSA at 4°C overnight at the following dilutions: mouse anti-Brp (NC82):1/100; mouse Dlg (4F3): 1/100; mouse anti-Eve (3C10): 1/10; obtained from Developmental Studies Hybridoma Bank (University of Iowa); rabbit anti-GFP (A-11122, Invitrogen): 1/1000, goat anti-HRP Cy3 (Jackson ImmunoResearch Laboratories): 1/800; mouse anti-KIF5A (Santa Cruz Biotechnology sc-376452):1/500. Corresponding secondary antibodies were incubated for 2 h at room temperature: AlexaFluor-594 donkey anti-mouse, AlexaFluor-488 donkey anti-rabbit (Fisher Scientific) were used at 1/800 dilution. The larval fillet preparations were mounted in 80% glycerol.

**Image acquisition.** Imaging was performed on a Zeiss LSM880 Airyscan confocal microscope with a 63 $\times$  Plan Apo 1.4 numerical aperture objective. Laser intensity and gain were adjusted to increase the signal without overexposure. All images for the same experiment set were collected under identical conditions using identical imaging and processing parameters. All images were collected as 0.7  $\mu$ m (for NMJs) or 0.5  $\mu$ m (for ventral nerve cords [VNCs]) optical sections, and the *z* stacks were processed and analyzed with Fiji (National Institutes of Health). Representative images are the maximum projection of the corresponding confocal *z* stack; brightness and contrast were adjusted in Adobe Photoshop 2022 (Adobe System).

For the quantification of NMJ morphology (muscle 4 segments A3-A5), HRP staining was used to quantify NMJ area with Fiji software and axonal length with NeuronJ plugin. The number of Brp puncta was manually counted. For the quantification of the mitochondrial fluorescence intensity, at the NMJ (muscle 4, segments A3-A5) and proximal segmental nerve, *z*-stack NMJs stained by GFP and HRP were converted to maximum intensity projection using Fiji. HRP channel allowed delineation of the synaptic terminals or the nerve portion representing the area considered. A threshold mask was applied to the GFP channel and the RawIntDen, which represents the total intensity of GFP (Mito-GFP) signal, was calculated. For each genotype, the GFP intensity was normalized per unit area.

Pictures of larvae and adult flies were acquired with a Nikon camera (5 M pixels); images were processed with Adobe Photoshop 2022. Eye area was determined with the Fiji plugin.

**Electrophysiology.** Electrophysiological recordings were obtained, as previously described (Imlach and McCabe, 2009), from third-instar larvae at the wandering stage. Briefly, larvae were dissected in “free-Ca<sup>2+</sup>” HL3.1 solution (to avoid muscular contraction) containing the following (in mM): 70 NaCl, 5 KCl, 4 MgCl<sub>2</sub>, 10 NaHCO<sub>3</sub>, 5 trehalose, 115 sucrose, and 5 HEPES, pH 7.2. Electrophysiological experiments were then performed on larvae infused with HL3.1 solution containing 1 mM Ca<sup>2+</sup>. The cut end of the motor neuron was sucked into a patch pipet (resistance ~1 M $\Omega$ ) to apply local stimulation. Recordings from muscle 6, segment A3, were obtained with electrodes of a resistance of 30–40 M $\Omega$  filled with 3 M KCl, using an Axon Multiclamp 700B amplifier (Molecular Devices). Only muscles presenting a resting membrane potential <–60 mV and an input resistance of  $\geq$ 5 M $\Omega$  were considered. Data were analyzed using Clampfit.

The different electrophysiological protocols used were as follows: miniature excitatory junction potentials (mEJP) were recorded at resting potential for 3 min without any stimulation. From these recordings, resting potential and both mEJP amplitude and frequency could be determined. Evoked excitatory junction potentials (eEJPs) were obtained by applying 10 stimulations every 6 s, at voltage sufficient to induce muscle evoked responses (1–3 mV). An average of these recordings was obtained to determine eEJP parameter.

Quantal content was obtained by dividing the average amplitude of eEJPs by the average amplitude of mEJPs. Paired-pulse stimuli protocols, consisting of applying 2 consecutive pulses (at 20 or 50 Hz), were performed to study synaptic facilitation. Quantification was obtained by dividing the amplitude of the second eEJP (A2) by the amplitude of the first eEJP (A1). Activity-dependent fatigue of neurotransmitter release was studied by recording multipulse protocols of either 100 consecutive stimulations (at 20 and 50 Hz) or 200 consecutive stimulations at 10 Hz. Quantification was obtained by dividing the amplitude of the last eEJP (A100 or A200) by the amplitude of the first eEJP (A1), respectively. The number of larvae studied is given.

**Negative geotaxis assay.** Ten males from VGlut-Gal4; tub-Gal80<sup>ts</sup> X UAS KIF5A WT or KIF5A  $\Delta$ 27 or control crosses, reared at 29°C from hatching, were assayed at 3 or 10 d old for climbing. They were placed in 25 ml Falcon pipet and allowed to recover. Each pipet was assayed by tapping the flies down to the bottom of the pipet, and the number of flies that climbed above 12 cm mark within 30 s was counted. This assay was repeated twice, with a rest period of 2 min between each trial. The number of flies that passed the 12 cm mark was expressed as a percentage of the total flies.

**Lifespan analysis.** Lifespan experiments were done at 29°C. VGlut-Gal4, tub-Gal80<sup>ts</sup> flies were crossed to UAS KIF5A WT or  $\Delta$ 27 transgenes or the control line. The crosses were maintained at the permissive temperature of 18°C. The progeny of these crosses was collected; 20 males per tube were placed at 29°C to age. Food was changed every 2–3 d and the number of dead flies was recorded.

**Experimental design and statistical analyses.** For all experiments, the control and experimental genotypes were tested at the same time.

Values were tested for normal distribution using a D’Agostino and Pearson test. Statistical differences between two experimental groups were assessed using the Mann–Whitney test or unpaired *t* test. For multiple comparisons, one-way ANOVA with Tukey’s *post hoc* test was used for statistical analysis. For nonparametric values, a Kruskal–Wallis test was applied with a Dunn’s *post hoc* test. For the longevity assays, Kaplan–Meier survival curves were generated, and significant differences were assessed based on the log-rank (Mantel–Cox) test. All statistical analyses were performed using GraphPad Prism (version 9). In all figures, error bars indicate the mean  $\pm$  SD. The number of samples tested (*n*) is given in the figure legends.

## Results

### KIF5A $\Delta$ 27 expression induces pathogenicity in *Drosophila*

The vast majority of KIF5A mutations found in ALS patients affect the splicing sites of exon 27 leading to its skipping

(Brenner et al., 2018; Nicolas et al., 2018). This results in a mutated protein, called KIF5A  $\Delta$ 27, with an aberrant C-terminal tail because of translational frameshifting (Fig. 1A). To investigate the effects of ALS-related KIF5A mutant *in vivo*, we generated transgenic lines to express KIF5A in different tissues using the UAS-Gal4 expression system (Brand and Perrimon, 1993).

First, we tested the effects of KIF5A expression in the adult fly eye, a convenient model to explore cellular toxicity in neurodegenerative diseases (Bilen and Bonini, 2005). The *Drosophila* eye is composed of ~800 unit eyes called ommatidia, organized in a stereotyped manner. Any slight disturbance leads to morphologic changes that result in a visible phenotype. To assess the effect of the WT or mutated form of KIF5A in the eyes, we used the GMR-Gal4 driver, which allows UAS transgene to be expressed in the developing eyes (Freeman, 1996). We verified that, when expressed under the control of GMR-Gal4, the WT and pathogenic forms of KIF5A were expressed comparably in the two transgenic lines (Fig. 1B,C). When KIF5A  $\Delta$ 27 is expressed, flies present smaller eyes compared with the control and flies expressing the WT form of KIF5A (Fig. 1D,E). This observation strongly suggests that ALS-associated KIF5A mutant confers cellular toxicity. To confirm this result, we used another genetic system that controls the wing expansion of newly adult eclosed flies. Crustacean cardioactive peptide (CCAP) neurons control posteclosion behavior, including wing expansion and cuticle tanning (Park et al., 2003). Expression of KIF5A  $\Delta$ 27 under the control of CCAP-Gal4 resulted in adult flies with poorly or completely unexpanded wings compared with control flies or flies that express the WT form of KIF5A (Fig. 1F,G). These data show that the expression of the ALS-associated KIF5A  $\Delta$ 27 mutant, but not the KIF5A WT, leads to toxicity in neuronal cells.

### Expression of ALS-linked KIF5A mutant in motor neurons leads to locomotor deficits and alterations of NMJ morphology

We next sought to investigate the locomotor behavior of larvae expressing the WT or the mutated form of KIF5A selectively in motor neurons using the VGlut-Gal4 driver (Mahr and Aberle, 2006). A lower expression of KIF5A  $\Delta$ 27 was observed compared with that of KIF5A WT in the larval CNS when assayed by Western blot experiments (Fig. 2A,B). Even so, at the behavioral level, compared with control flies, the expression of both forms of KIF5A induced a decrease in the traveled distance (Fig. 2C). However, the effect of KIF5A  $\Delta$ 27 on larval locomotion is more severe than that of KIF5A WT. This finding is corroborated by analyzing the posture of these larvae on a substrate surface. While control and KIF5A WT-expressing larvae remained flat with all segments adhering to the surface, larvae expressing KIF5A  $\Delta$ 27 in motor neurons exhibited a “tail-flip” phenotype (Fig. 2D,E). This phenotype is produced by an upward tilt of the posterior larval segments after each peristaltic wave of muscle contraction, likely because of paralysis of the posterior segments (Hurd and Saxton, 1996; Martin et al., 1999). This tail-flipping phenotype is characteristic and is one of the hallmarks of axonal transport defects in motor neurons (Hurd and Saxton, 1996; Martin et al., 1999).

We then analyzed the morphology of the NMJ of larvae expressing KIF5A WT or mutant in motor neurons. Anti-HRP staining was used to visualize the synaptic overall NMJ area (Menon et al., 2013). The number of active zones (AZs), the release sites of synaptic vesicles, was determined through the presence of Bruchpilot (Brp), an essential structural component of the AZs (Wagh et al.,

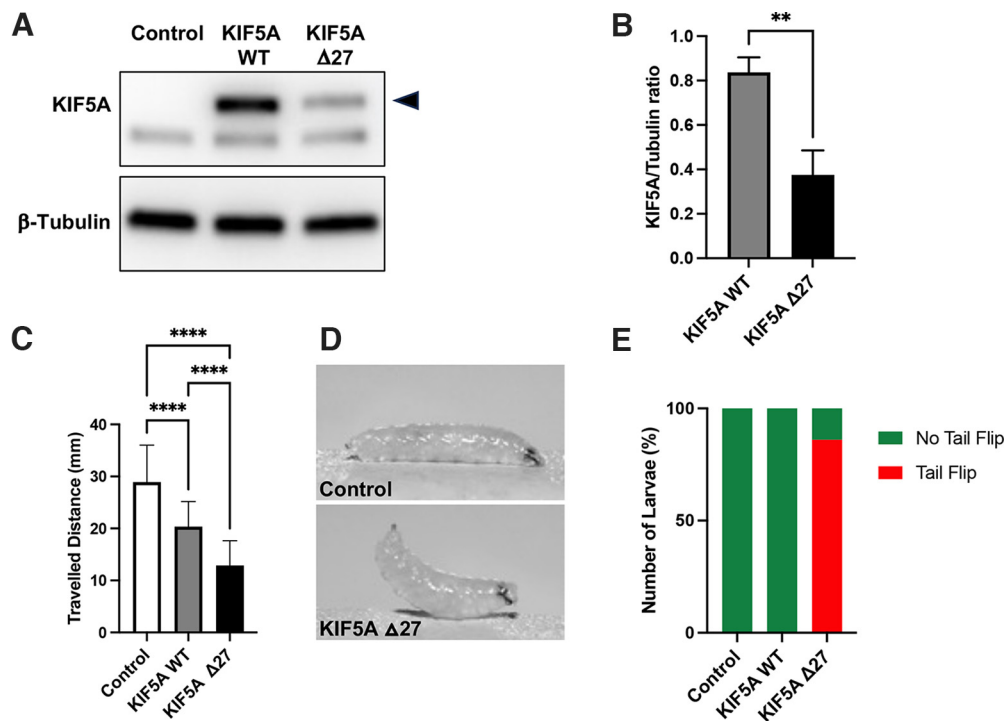


**Figure 2.** Expression of KIF5A  $\Delta$ 27 in motor neurons leads to locomotion defects. **A**, Extraction of total protein was performed from dissected CNS of control (VGlut-Gal4/+), KIF5A WT (VGlut-Gal4/UAS-KIF5A WT), and KIF5A  $\Delta$ 27 (VGlut-Gal4/UAS-KIF5A  $\Delta$ 27) expressing larvae. Top, Anti-KIF5A staining (black arrowhead). Bottom, Anti- $\beta$ -tubulin, used as a loading control. **B**, Quantification of gel bands was done by using Fiji software (Analyze gels); five gels were analyzed. Data are mean  $\pm$  SD.  $**p < 0.01$  (Mann-Whitney test). **C**, The crawling behavior is studied on control and larvae expressing either KIF5A WT or KIF5A  $\Delta$ 27 in motor neurons using the VGlut-Gal4 driver. Expression of KIF5A WT significantly reduces the traveled distance compared with control. However, expression of the ALS-related form of KIF5A even more significantly reduces the locomotor behavior compared with control and KIF5A WT-expressing larvae ( $n = 64, 56$ , and  $59$  for control, KIF5A WT, and KIF5A  $\Delta$ 27, respectively). Data are mean  $\pm$  SD.  $****p < 0.0001$  (one-way ANOVA with Tukey *post hoc* test). **D**, When placed on a substrate, control larvae (top) adhere and maintain a flat body posture. Larvae expressing KIF5A  $\Delta$ 27 in motor neurons under the control of VGlut-Gal4 driver exhibit a paralysis of the posterior segments known as “tail-flip” phenotype (bottom). **E**, Quantification of individuals with indicated phenotype shows that 86% of larvae expressing KIF5A  $\Delta$ 27 exhibit a tail-flip phenotype, while control and KIF5A WT-expressing larvae do not ( $n = 50$  for each genotype).

2006). Surprisingly, KIF5A WT expression increased both NMJ length and area compared with the control condition (Fig. 3A–C). However, the number of AZs present relative to the NMJ area measurement (or relative to the number of boutons) remained constant, indicating that the number of AZs is stable and adapted to the total NMJ length (Fig. 3A,D,E). This overgrowth phenotype may be because of a compensatory mechanism at the synaptic level to adapt to the locomotor defect. We then analyzed the NMJ morphology of larvae that expressed KIF5A  $\Delta$ 27 in motor neurons and found that it was strongly altered. Indeed, the total axonal length of the NMJ branches is diminished, as well as the surface area of the NMJs (Fig. 3A–C). The number of AZs in KIF5A  $\Delta$ 27 larvae is also significantly reduced compared with the control and KIF5A WT-expressing larvae (Fig. 3A,D,E). These results are consistent with the drastic reduction in locomotor ability of larvae expressing KIF5A  $\Delta$ 27 compared with control and KIF5A WT larvae.

We then asked whether the postsynaptic apparatus of the NMJ might be affected by KIF5A mutant. We examined the labeling of Discs-large (Dlg), a marker of the subsynaptic reticulum (SSR) that forms numerous layers of invaginated membrane surrounding the presynaptic terminals (Budnik et al., 1996). Regardless of the form of KIF5A expressed in motor neurons, the presynaptic terminals are always closely apposed to the SSR Dlg labeling, as observed in control larvae (Fig. 3F). This result shows that KIF5A expression in motor neurons did not affect the postsynaptic part of the NMJ.

The severe reduction in locomotion observed in larvae expressing KIF5A  $\Delta$ 27 in their motor neurons is correlated with

a significant shortening of the size of the NMJs and a decrease in the number of AZs. Together, these data strongly suggest that the expression of KIF5A  $\Delta$ 27 is detrimental to motor neurons.

### Expression of KIF5A $\Delta$ 27 in motor neurons impairs synaptic transmission

Since KIF5A  $\Delta$ 27 expression in motor neurons affects locomotor behavior and NMJ morphology, we asked whether KIF5A  $\Delta$ 27 may generate physiological alterations in larval motor neurons. We recorded the mEJPs at rest and eEJPs to assess postsynaptic transmission at the NMJ. We found that the expression of KIF5A  $\Delta$ 27 in motor neurons led to a decrease in mEJP amplitude and frequency compared with the control (Fig. 4A–C). In addition, the amplitude of the eEJP and the quantal content were strongly reduced by KIF5A  $\Delta$ 27 expression in motor neurons (Fig. 4A,D,E). Importantly, the expression of KIF5A WT in motor neurons did not affect spontaneous or evoked synaptic transmission compared with the control (Fig. 4A–E). Thus, KIF5A  $\Delta$ 27, but not KIF5A WT, impairs synaptic transmission at NMJs. We next challenged the synaptic release machinery of KIF5A-expressing motor neurons using high-frequency stimulations (Kauwe and Isacoff, 2013; Newman et al., 2017). We found that motor neurons expressing either KIF5A WT or KIF5A  $\Delta$ 27 were unable to sustain 20 Hz stimulations compared with the control condition (Fig. 4F,G). A gradual time-dependent decrease in eEJP amplitude was observed, as shown by the ratio of the amplitude measured at the first stimulation to the second or the hundredth (Fig. 4F,G). Similarly,

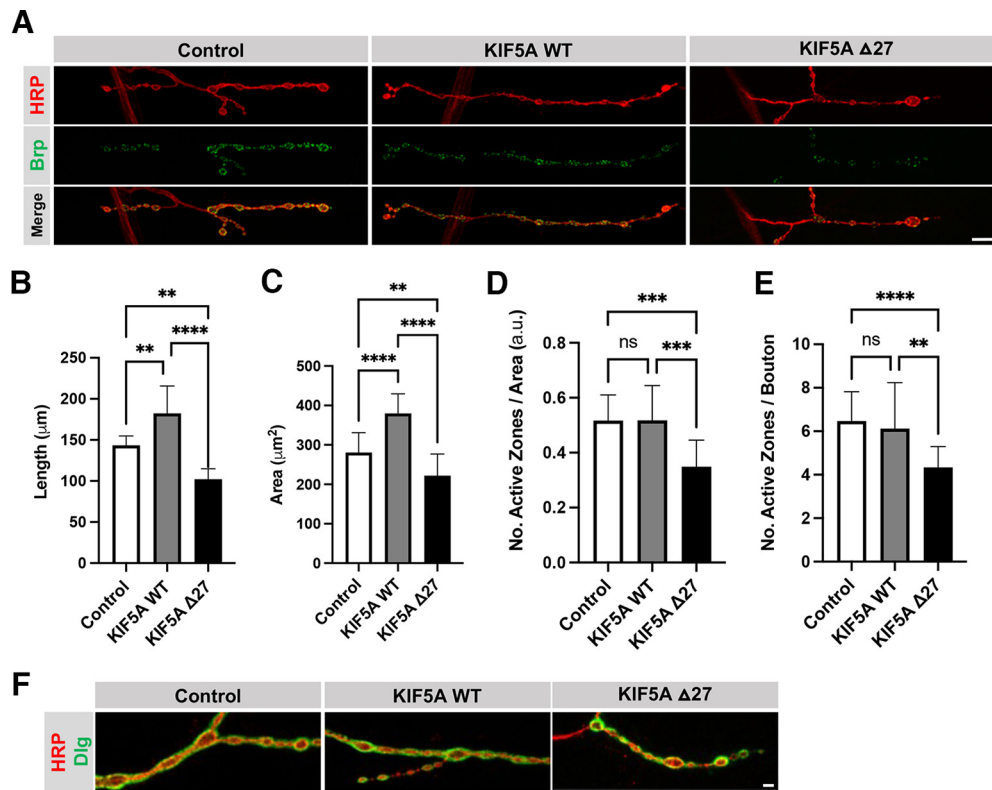


**Figure 3.** The morphology of the NMJs is affected by KIF5A  $\Delta$ 27 expression in motor neurons. **A**, NMJs from control third instar larvae (VGlut-Gal4/+ ) or expressing KIF5A WT or  $\Delta$ 27 are visualized using the neuronal membrane marker anti-HRP (red). AZs are labeled with anti-Brp (green). KIF5A  $\Delta$ 27 expression in motor neurons induces a decrease in both the NMJ size and the number of AZs. NMJs innervating the muscle 4 of segment A3–A5 are shown. Scale bar, 50  $\mu\text{m}$ . **B–E**, Quantification of the total length of NMJ axonal branches (**B**), NMJ area (**C**), numbers of AZs/area of NMJ (**D**), and AZs/bouton (**E**). The number of NMJs observed for VGlut-Gal4/+, VGlut-Gal4/KIF5A WT, and VGlut-Gal4/KIF5A  $\Delta$ 27 is 16, 19, and 15, respectively. Data are mean  $\pm$  SD. a.u., arbitrary units. ns,  $p > 0.05$ ; \*\* $p < 0.01$ ; \*\*\* $p < 0.001$ ; \*\*\*\* $p < 0.0001$ ; Kruskal–Wallis test and Dunn’s multiple comparison test. **F**, Presynaptic and postsynaptic parts of the NMJs are visualized using the neuronal membrane marker HRP (red) and the postsynaptic density marker Dlg (green), respectively, in control and in larvae expressing KIF5A WT or KIF5A  $\Delta$ 27. Scale bar, 20  $\mu\text{m}$ .

when a higher (50 Hz) or lower (10 Hz) stimulation frequency was applied, the synaptic capacity to respond in a sustained manner was impaired by the expression of both WT and mutated KIF5A (Fig. 5). Collectively, these results show that synaptic neurotransmission at the NMJ level is significantly disrupted by KIF5A  $\Delta$ 27 expression in motor neurons. This is consistent with the altered locomotor behavior and pathogenic effect observed upon KIF5A  $\Delta$ 27 expression.

### KIF5A $\Delta$ 27 leads to mitochondria and synaptic vesicle aggregates in motor neurons

KIF5A is involved in the anterograde transport of mitochondria from the soma to the synapse. Therefore, we studied the distribution of mitochondria in the cell body, axon, and NMJ of larval motor neurons using the Mito-GFP reporter line. This UAS construct allows the expression of GFP fused to a mitochondrial import sequence, allowing mitochondria visualization (Pilling et al., 2006).

In control motor neurons, numerous and uniformly distributed mitochondria are found in the soma, axons, and NMJs (Fig. 6A). In motor neurons expressing KIF5A WT, we observed an increase in the area-normalized intensity of mitochondria-related fluorescence in the cell bodies and axons, accompanied by a decrease intensity at the NMJs (Fig. 6A–D). In KIF5A  $\Delta$ 27-expressing motor neurons, mitochondria form large inclusions in the cell bodies and axons (Fig. 6A), resulting in a significant decrease in the axons of the mean mitochondria-related

fluorescence intensity expressed relative to total area (Fig. 6C). Moreover, we observed that the synaptic bouton content of mitochondria at the NMJs is significantly reduced in KIF5A  $\Delta$ 27-expressing motor neurons (Fig. 6D).

We also asked whether KIF5A  $\Delta$ 27 expression might affect the distribution of synaptic vesicles. In control or KIF5A WT-expressing motor neurons, vesicles labeled using the neuropeptide Y (NPY)-GFP construct (Mudher et al., 2004), are homogeneously distributed in the axons up to the NMJs (Fig. 6E,F). Conversely, KIF5A  $\Delta$ 27 expression induces the formation of vesicle clusters in the axons. In addition, the fluorescence intensity related to the amount of synaptic vesicles present at the NMJs is strongly decreased compared with the control condition or KIF5A WT expression (Fig. 6E,F).

Together, these results show that the ALS-linked KIF5A mutant leads to aggregates of mitochondria and synaptic vesicles along motor neuron axons, which might explain the reduction in NMJ size and the alteration of synaptic neurotransmission previously observed.

### ALS-associated KIF5A mutant is found in cytoplasmic inclusions and induces axonal damage

We also studied the localization of KIF5A in axons and found that KIF5A WT is homogeneously distributed along the larval nerves in contrast to KIF5A  $\Delta$ 27, which forms cytoplasmic inclusions (Fig. 7A). Furthermore, the tendency of KIF5A  $\Delta$ 27 to aggregate is very high, as cytoplasmic inclusions were found in all

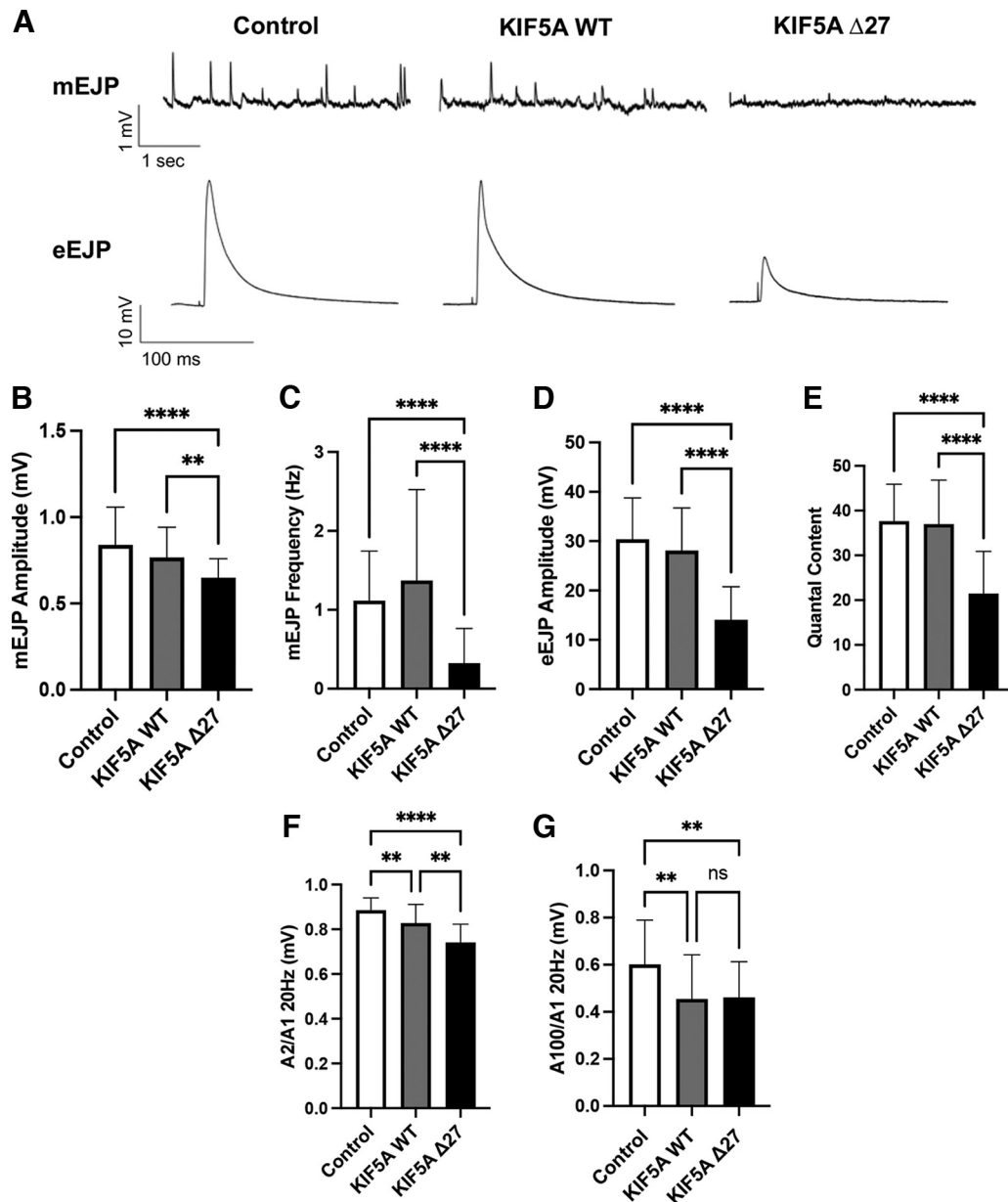


**Figure 4.** Synaptic neurotransmission is impaired in motor neurons expressing ALS-related KIF5A. **A**, Representative traces showing mEJPs (top) and eEJPs (bottom) in control and in larvae expressing either KIF5A WT or KIF5A  $\Delta$ 27 in motor neurons using VGlut-Gal4 driver. **B**, **C**, Amplitude (**B**) and frequency (**C**) of mEJPs recorded in the muscle 6 of control, KIF5A WT, and KIF5A  $\Delta$ 27 larvae. **D**, Amplitude of eEJPs recorded in the muscle 6 of larvae of the different indicated genotypes. The amplitude of eEJPs is strongly decreased upon KIF5A  $\Delta$ 27 expression compared with control and KIF5A WT-expressing larvae. **E**, Histogram represents the mean quantal content for control, KIF5A WT, and KIF5A  $\Delta$ 27-expressing larvae. The quantal content is calculated by dividing the mean eEJP by the mean mEJP. **B–E**,  $n = 51$ , 37, and 46 larvae recording for control, KIF5A WT, and KIF5A, respectively.  $**p < 0.01$ ;  $****p < 0.0001$ ; Kruskal–Wallis test and Dunn’s *post hoc* test. **F**, **G**, NMJs were subjected to a train of 100 stimulations at a frequency of 20 Hz. The amplitude of the first response (A1) is measured and compared with the amplitude of the second stimulation (A2) to obtain the A2/A1 ratio and to the 100th (A100) to obtain the A100/A1 ratio, respectively. The response of larvae expressing KIF5A WT or KIF5A  $\Delta$ 27 is decreased compared with the control. Recordings were made from 39, 36, and 26 control, KIF5A WT, and KIF5A  $\Delta$ 27 larvae, respectively. Data are mean  $\pm$  SD. ns,  $p > 0.5$ ;  $**p < 0.01$ ;  $****p < 0.0001$ ; Kruskal–Wallis test and Dunn’s *post hoc* test or ordinary one-way ANOVA and Tukey *post hoc* test (**F**).

observed nerves, whereas only 10.7% of nerves showed aggregates when KIF5A WT is expressed (Fig. 7B). Strikingly, we noticed that KIF5A  $\Delta$ 27, but not KIF5A WT, disturbs the distribution of the coexpressed cytoplasmic GFP in motor neurons. Axonal swelling is observed with cytoplasmic GFP showing diffuse localization and forming clusters, some of which are colocalized with KIF5A inclusions (Fig. 7A, white arrowheads). To further confirm that axonal integrity is affected by KIF5A  $\Delta$ 27, we used HRP staining to label the membranes of axonal motor neurons. Compared with the uniform distribution of HRP labeling

in control and KIF5A WT-expressing motor neurons, HRP labeling of motor neurons expressing KIF5A  $\Delta$ 27 reveals numerous HRP-positive aggregates and a decrease in labeling intensity (Fig. 7C). This result reinforces the idea that the integrity of the axons is disrupted by KIF5A  $\Delta$ 27 expression. Importantly, we also found numerous KIF5A  $\Delta$ 27-positive inclusions in the cell bodies of motor neurons, whereas KIF5A WT is uniformly distributed (Fig. 7D,E). Together, these data show that KIF5A  $\Delta$ 27 is found in cytoplasmic inclusions that trap cytoplasmic GFP as well as some HRP-positive components.

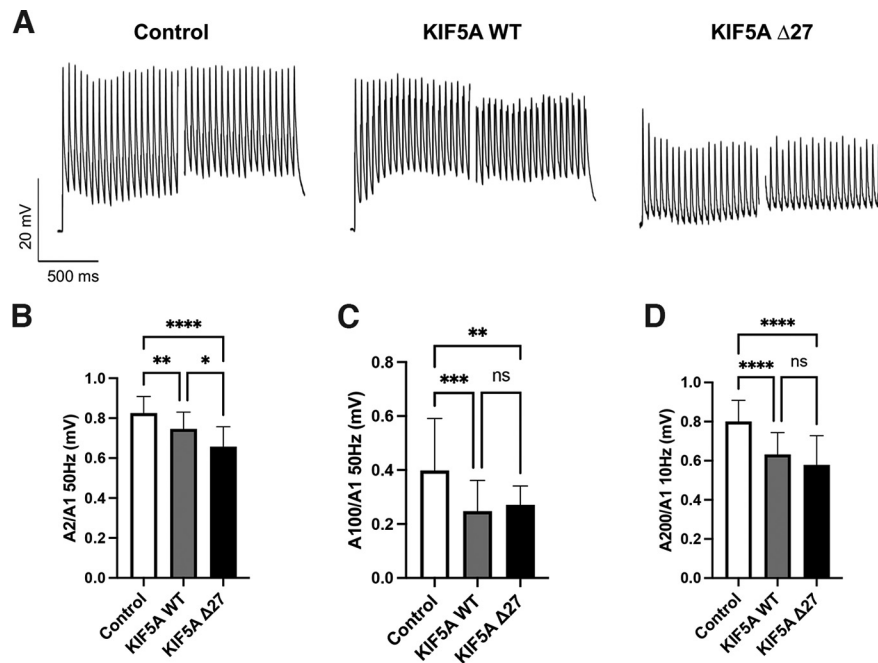


**Figure 5.** High-frequency response is impaired in motor neurons expressing KIF5A. **A**, Representative traces of 20 Hz stimulation recordings at the NMJ of control or motor neurons expressing either KIF5A WT or KIF5A  $\Delta$ 27. **B**, **C**, Train stimulations performed at 50 Hz. Motor neurons expressing KIF5A  $\Delta$ 27 are unable to maintain a response amplitude similar to control from the second stimulation as shown by the A2/A1 ratio (**B**); the defect is amplified after the 100th stimulation (**C**). The same defect is observed upon KIF5A WT expression but to a lesser extent after the second stimulation (**B**). Recordings were made in **B** from 31, 29, and 21 control, KIF5A WT, and KIF5A  $\Delta$ 27 larvae, respectively, and in **C** from 28, 31, and 21 control, KIF5A WT, and KIF5A  $\Delta$ 27 larvae, respectively. **D**, Protocol of long stimulations at 10 Hz. Motor neurons expressing KIF5A WT or  $\Delta$ 27 are unable to maintain a response amplitude similar to control as shown by the A200/A1 ratio. Recordings were made from 21, 24, and 16 control, KIF5A WT, and KIF5A  $\Delta$ 27 larvae, respectively. Data are mean  $\pm$  SD. Significance was assessed using the Kruskal–Wallis test and Dunn’s *post hoc* test (**B**) or ordinary one-way ANOVA and Tukey *post hoc* test (ns,  $p > 0.5$ ; \* $p < 0.1$ ; \*\* $p < 0.01$ ; \*\*\*\* $p < 0.0001$ ).

### KIF5A $\Delta$ 27 leads to the loss of motor neurons and a shorter life span

We asked what the consequences of these KIF5A mutant-induced cellular abnormalities might be on the survival of motor neurons. The organization of motor neuron cell bodies is stereotyped and patterned in the larval VNC. Interestingly, we observed that this organization appears to be altered on KIF5A  $\Delta$ 27 expression, suggesting that motor neuron loss may occur. Thus, we decided to take a closer look at the cell bodies of these motor neurons. To this end, we followed the aCC and RP2 motor neurons, located in the dorsal part of the VNC and expressing the Even-skipped (Eve) transcription factor. We focused on this subpopulation of motor neurons because they are easy to distinguish and count because of their reproducible pattern in the different segments of the VNC (Landgraf et al., 2003). We observed a decrease in the number of Eve-positive motor neurons per segment on KIF5A  $\Delta$ 27 expression (Fig. 8A,B), which leads to an overall disorganization of the motor neuron cell bodies in the different segments of the VNC. This result shows that the expression of KIF5A  $\Delta$ 27 is pathogenic in motor neurons and leads to their loss. However, the KIF5A mutant-induced pathogenicity did not affect the viability of the larvae reared at the conventional temperature of 25°C, as viable adult flies emerged. We decided to sensitize the system and breed the *Drosophila* vials at 29°C, a temperature that increases both the developmental rate and the activation of the UAS-Gal4 system (Brand et al., 1994). Under these conditions, KIF5A  $\Delta$ 27 induces drastic lethality, with larvae dying throughout the larval stage with very few pupae formed (Fig. 8C,D). Importantly, control and KIF5A WT-expressing *Drosophila* emerge similarly to adult flies at 29°C.

We next asked whether the expression of KIF5A  $\Delta$ 27, at the adult stage, would influence adult life expectancy and motor

functions of flies. We first ensured that the expression levels of KIF5A transgenes using VGlut-Gal4 in adult VNC were similar (Fig. 9A,B). Then, we took advantage of the tub-Gal80<sup>ts</sup> construct combined with the VGlut-Gal4 driver to allow induction of KIF5A  $\Delta$ 27 or WT only at the adult stage by shifting the temperature to 29°C. We measured the life-span of males by counting the number of flies dead every 2–3 d. We found that expression of KIF5A  $\Delta$ 27, selectively in adult motor neurons, decreased lifespan (Fig. 9C). A 25% reduction of lifespan was observed in KIF5A  $\Delta$ 27-expressing flies compared with control, with a median survival of 15 and 20 d, respectively. A lifespan effect was also observed in the KIF5A WT condition, with a median survival of 22 d. Next, we analyzed the motor activity of these animals using a negative geotaxis assay. Negative geotaxis is the ability of a fly to move vertically when startled; it is based on an innate escape response during which after being tapped to the bottom of a pipet the flies ascend the wall (Martinez et al., 2007). We chose to assay the motor activity of males at 3 d, shortly after their shift to 29°C, and at 10 d (i.e., before they reached their half-life). At 3 d, no significant difference was observed between the different genotypes. Indeed, males expressing KIF5A  $\Delta$ 27 in motor neurons have a comparable climbing ability to the control or males expressing KIF5A WT (Fig. 9D). However, 10 d after being placed at 29°C, males expressing KIF5A  $\Delta$ 27 in motor neurons exhibited a significant 70% reduction in their climbing ability compared with control or males expressing KIF5A WT (Fig. 9D).

These results indicate that, in contrast to the expression of the WT form of KIF5A, the expression of KIF5A  $\Delta$ 27 is deleterious to motor neurons in both larvae and adults and reduces the life expectancy of adult flies.



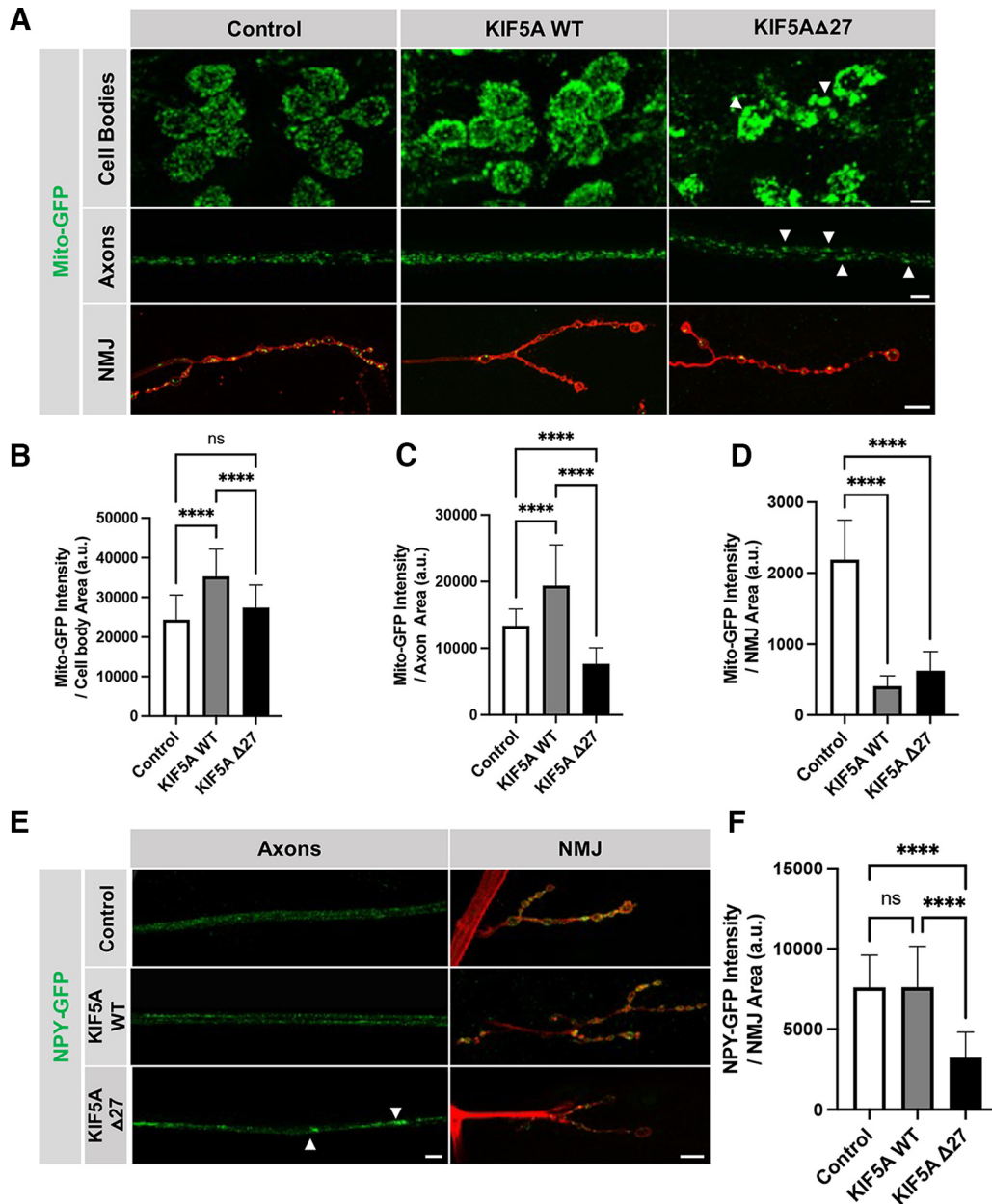


**Figure 6.** Mitochondria and synaptic vesicles form inclusions in motor neurons expressing KIF5A  $\Delta$ 27 mutant. **A**, KIF5A WT or  $\Delta$ 27 is expressed under the control of VGlut-Gal4, UAS Mito-GFP to label neuronal mitochondria. Mitochondria (green) are observed in the cell bodies, the proximal axons, and at the NMJs (labeled by HRP staining in red). In the soma and axon of control motor neurons, mitochondria are evenly distributed, whereas they are more densely packed upon KIF5A WT expression. Mitochondrial inclusions are found both in the cell bodies and in the axons of motor neurons expressing KIF5A  $\Delta$ 27 (white arrowheads). At the NMJs of control flies, mitochondria are found in the synaptic boutons. Fewer mitochondria are visible at the NMJs of larvae expressing either KIF5A WT or KIF5A  $\Delta$ 27. Scale bars, 50  $\mu$ m. **B–D**, Quantification of the fluorescence intensity of mitochondria relative to the cell body surface (**B**), axons (**C**), or NMJ (**D**) is reported for the different genotypes. Number of cell bodies observed,  $n = 87$ , 99, and 84 for the control, KIF5A WT, and KIF5A  $\Delta$ 27, respectively. Number of nerves observed,  $n = 22$ , 24, and 30 for the control, KIF5A WT, and KIF5A  $\Delta$ 27, respectively. Number of NMJs considered,  $n = 21$ , 25, and 18 for the control, KIF5A WT, and KIF5A  $\Delta$ 27, respectively. Data are mean  $\pm$  SD. a.u., arbitrary units. Significance is assessed using the Kruskal–Wallis test and Dunn’s *post hoc* test (**B**) or ordinary one-way ANOVA and Tukey *post hoc* test (**C,D**) (ns,  $p > 0.5$ ; \*\*\*\* $p < 0.0001$ ). **E**, Axons and NMJs of VGlut-Gal4, UAS NPY-GFP (control) larvae expressing either KIF5A WT or  $\Delta$ 27 mutant are shown. The GFP staining (green) labels the synaptic vesicles loaded into proximal axons and NMJs. In the axons, the distribution of the synaptic vesicles is homogeneous in control as well as in KIF5A WT expression condition. Expression of KIF5A  $\Delta$ 27 disturbs the synaptic vesicle distribution, and aggregates are present along the axon (arrowheads). At the NMJs, costained by anti-HRP (red), the synaptic vesicles (green) are found in the different boutons in control larvae and in larvae expressing KIF5A WT. On the contrary, a significant decrease of the GFP fluorescence intensity is observed at the NMJs upon KIF5A  $\Delta$ 27 expression. Scale bar, 40  $\mu$ m. **F**, Quantification of the intensity of GFP fluorescence related to the NMJ area. Number of NMJs considered,  $n = 17$ , 16, and 17 for control, KIF5A WT, and KIF5A  $\Delta$ 27, respectively. Data are mean  $\pm$  SD. a.u., Arbitrary units. ns,  $p > 0.5$ ; \*\*\*\* $p < 0.0001$ ; one-way ANOVA and Tukey’s test.

## Discussion

With the aim of deciphering the cellular and molecular mechanisms altered by the expression of ALS-associated KIF5A mutant, we developed a *Drosophila* model based on KIF5A  $\Delta$ 27 expression selectively in motor neurons. Our data show that the

KIF5A mutant is highly detrimental to motor neurons. Indeed, KIF5A  $\Delta$ 27 alters morphology and synaptic transmission at larval NMJs. These defects are associated with disturbed locomotion and a tail-flip phenotype that is characteristic of axonal transport defects. Concordantly, KIF5A  $\Delta$ 27 is found in cytoplasmic inclusions in

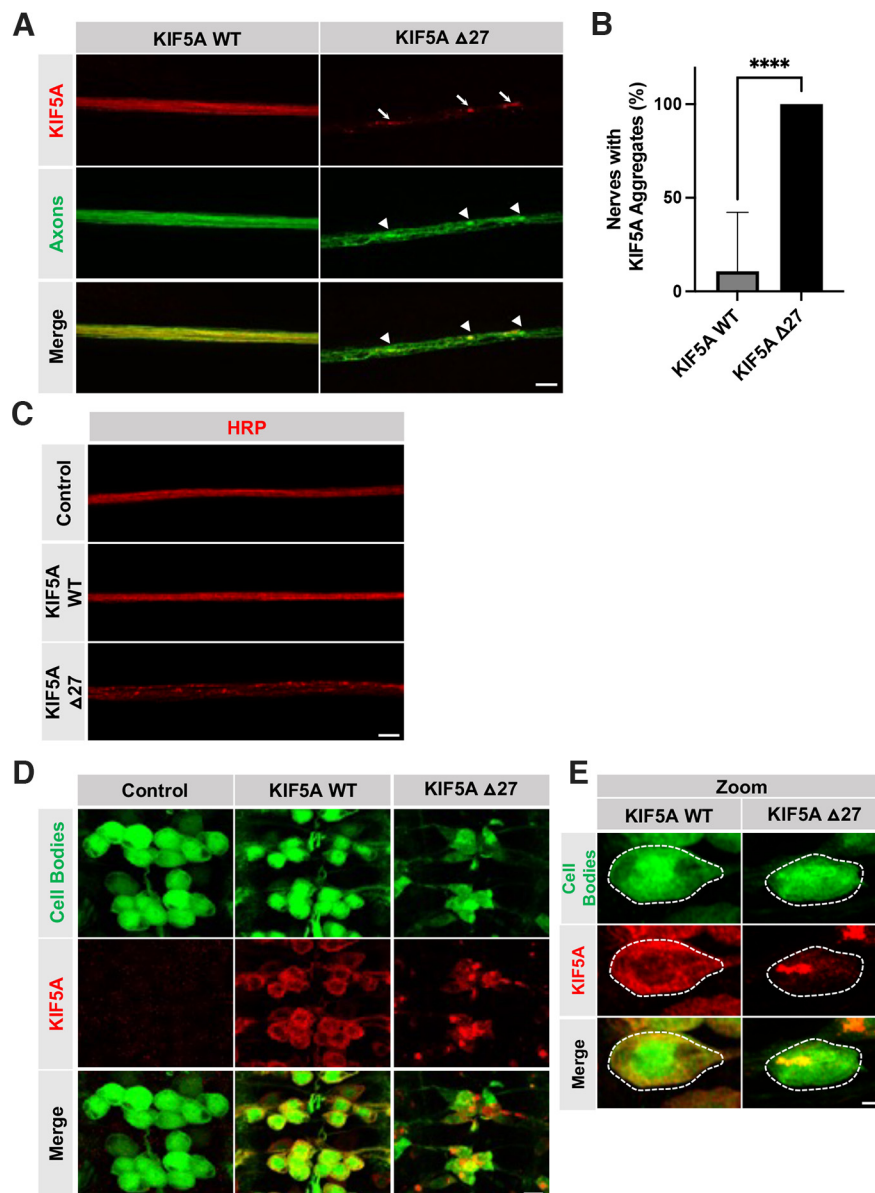


**Figure 7.** KIF5A  $\Delta$ 27 forms cytoplasmic inclusions and induces axonal damage. **A**, Coimmunostainings with anti-KIF5A (red) and anti-GFP (green) on motor neuron axons of VGlut-Gal4, UAS-GFP, UAS-KIF5A larvae. In axons expressing KIF5A WT, KIF5A is uniformly distributed. On the contrary, KIF5A  $\Delta$ 27 is found scattered and in cytoplasmic inclusions along axons (white arrows). KIF5A  $\Delta$ 27-positive inclusions also contain GFP-positive inclusions (white arrowheads). Scale bar, 50  $\mu$ m. **B**, While a small percentage (10%) of motor neuron axons displays KIF5A WT containing inclusions, all observed motor neuron axons contain KIF5A  $\Delta$ 27-positive cytoplasmic inclusions. This strongly suggests that the ALS-related form of KIF5A is prone to aggregation. The number of axon-containing nerves observed is  $n = 27$  and 28 for KIF5A WT and KIF5A  $\Delta$ 27, respectively. Data are mean  $\pm$  SD. \*\*\*\* $p < 0.0001$  (Mann-Whitney test). **C**, Immunostaining with anti-HRP (red) on motor neuron axons from control (VGlut-Gal4/+) and larvae expressing either KIF5A WT or  $\Delta$ 27. HRP staining allows visualization of axonal membranes. In control and KIF5A WT-expressing larvae, the axonal membranes are uniformly stained by the HRP labeling. In contrast, HRP labeling is scattered and found in inclusions upon KIF5A  $\Delta$ 27 expression. Scale bar, 50  $\mu$ m. **D**, Cell bodies of motor neurons from VGlut-Gal4, UAS-GFP (control) larvae expressing either KIF5A WT or  $\Delta$ 27. GFP staining (green) allows visualization of the entire cell bodies. KIF5A WT (red) is uniformly localized in the cytoplasm, whereas KIF5A  $\Delta$ 27 is mostly found in cytoplasmic inclusions. Scale bar, 50  $\mu$ m. **E**, High-magnification view of a VGlut-Gal4, UAS-GFP, UAS KIF5A WT or  $\Delta$ 27 motor neuron cell body (outlined by a white dotted line) showing KIF5A  $\Delta$ 27 cytoplasmic inclusions (red). Scale bar, 50  $\mu$ m.

axons of motor neurons, along with abnormal clustering of mitochondria and synaptic vesicles. Together, our data show that KIF5A  $\Delta$ 27 mutant is associated with a toxic gain of function that could lead to motor neuronal death.

#### KIF5A $\Delta$ 27 ALS-related is associated with a toxic gain of function

Generalization of large-scale genomic studies by whole-exome sequencing or genome-wide association study analyses has led to the identification of a large number of new gene mutations in

various diseases. The biological interpretation of these variants that lack evidence of pathogenicity is a major objective for molecular diagnosis and to further increase our understanding of mechanisms leading to the pathology. Recently, different computational approaches showed that, unlike loss-of-function mutations that do not display a preferential location, gain-of-function mutations tend to cluster in spatial regions of the proteins. These regions are often protein interfaces involved in protein interactions with other molecules (Lelieveld et al., 2017; Gerasimavicius et al., 2022; Livesey and Marsh, 2022). Interestingly, KIF5A is a motor protein that bridges the microtubule rails and many

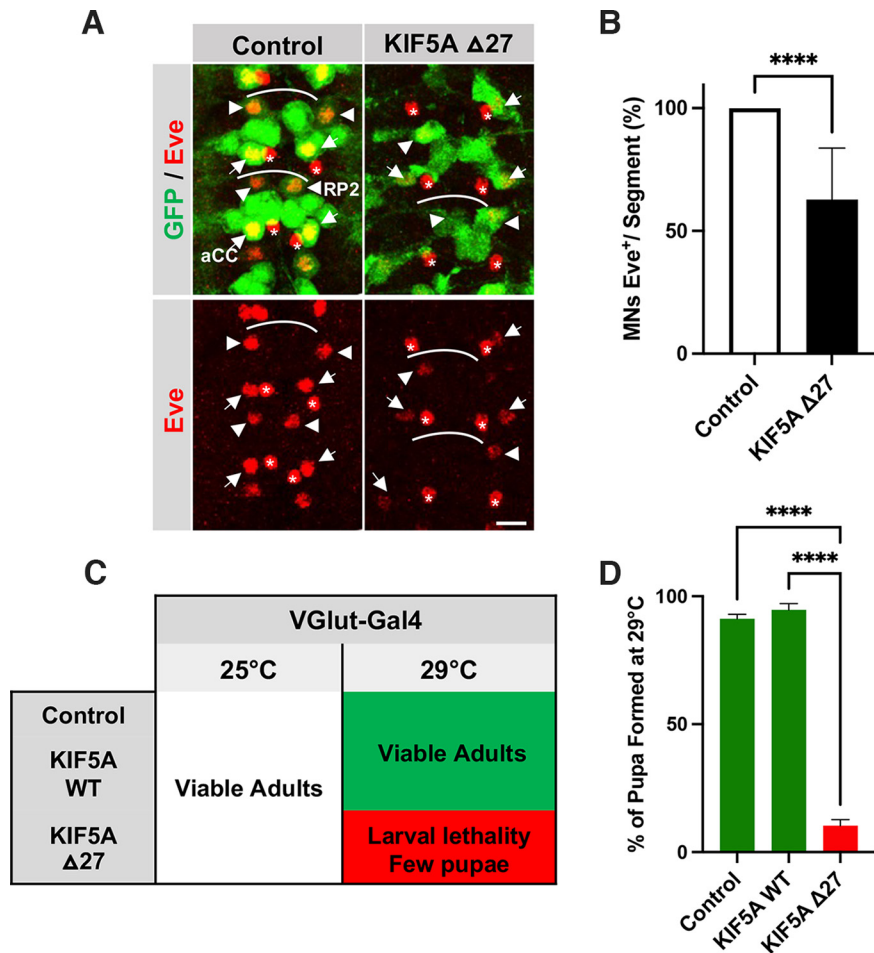


**Figure 8.** KIF5A  $\Delta$ 27 expression induces motor neuron loss and premature lethality. **A**, Left panels, The VNC of control VGlut-Gal4, UAS-GFP third instar larvae, costained with anti-Eve (red) and GFP (green). Motor neurons (green) in the dorsal part of the VNC are shown, with anterior up. In each segment (indicated by white lines), Eve labels a subpopulation of aCC (arrows) and RP2 (arrowheads) motor neurons as well as two pCC interneurons (marked with asterisks). Right panels, The expression of KIF5A  $\Delta$ 27 induced a loss of aCC and RP2 motor neurons. Scale bar, 50  $\mu$ m. **B**, Quantification of aCC/RP2 motor neuron number was performed in segments A5–A7. Expression of KIF5A  $\Delta$ 27 leads to a significant reduction (37.3%) in the number of motor neurons, indicating that KIF5A  $\Delta$ 27 is pathogenic. Number of segments counted  $n = 16$  and  $37$  for control and KIF5A  $\Delta$ 27, respectively. Data are mean  $\pm$  SD. \*\*\*\* $p < 0.0001$  (unpaired  $t$  test). **C**, At 25°C, expression of KIF5A WT or KIF5A  $\Delta$ 27 in motor neurons using the VGlut-Gal4 driver resulted in fully viable adults. At 29°C, KIF5A WT expression had no effect on the viability; adult flies eclosed as in the control. On the contrary, most larvae expressing KIF5A  $\Delta$ 27 died, and only 10.3% of them formed pupae that died at the pupal stage. **D**, The viability was determined by directly counting the number of larvae reaching the pupal stage at 29°C. Only 10.3% of pupae were present when KIF5A  $\Delta$ 27 was expressed in motor neurons compared to 91.2% and 94.7% in control and KIF5A WT conditions, respectively. Number of larvae considered:  $n = 250$ ,  $300$ , and  $300$  for the control, KIF5A WT, and KIF5A  $\Delta$ 27, respectively. Means  $\pm$  SD are expressed in percentages. \*\*\*\* $p < 0.0001$  (one-way ANOVA test with a Tukey *post hoc* test).

different cargos to ensure axonal transport from the soma to the periphery, allowing proper functioning of motor neurons. This central position implies that KIF5A interacts with various protein partners, making KIF5A a pivotal protein in motor neurons. Indeed, the mutations found in KIF5A are clustered mainly in the N- and C-terminal domains that connect the protein to microtubules and cargos, respectively. The pathologies associated with these mutations also follow this dichotomy (e.g., mutations located in the motor domain in the N-terminal part are linked to SPG10 a subtype of hereditary spastic paraplegia and CMT2 disorders) (Reid et al., 2002; L. Wang and Brown, 2010; Crimella et al., 2012; Fügler et al., 2012; Nam et al., 2018), while ALS-related mutations are clustered in the C-terminal part of the protein (Brenner et al., 2018; Nicolas et al., 2018).

ALS patients carrying the  $\Delta$ 27 mutation also have a WT copy of the KIF5A gene. Whether KIF5A  $\Delta$ 27 mutant causes ALS by a lack of functional kinesin via haploinsufficiency or by a gain-of-function effect remained elusive. Initially, the KIF5A  $\Delta$ 27 mutation was proposed as a loss of function (Nicolas et al., 2018). Results obtained in *cellulo* (Baron et al., 2022; Nakano et al.,

2022; Pant et al., 2022) and in our *Drosophila* model make it possible to reconsider the KIF5A  $\Delta$ 27 molecular mechanism underlying the pathogenicity in humans. Indeed, several reasons argue against haploinsufficiency of KIF5A function in ALS. First, mice lacking *Kif5A* die just after birth, while the loss of one copy of *Kif5A*, which results in a reduced amount of protein, is not deleterious (Xia et al., 2003; Karle et al., 2012). When cultured *in vitro*, *Kif5A*<sup>+/-</sup> motor neurons survived as well as control and did not show any defects in axonal and dendritic outgrowth compared with *Kif5A*<sup>-/-</sup> motor neurons (Karle et al., 2012). Importantly, the absence of defects in *Kif5A*<sup>+/-</sup> motor neurons is not because of compensatory mechanisms, as the expression of Kif5B and Kif5C is unchanged compared with the control (Xia et al., 2003). In *Drosophila*, the homologous gene of KIF5A is *khc*, which represents the only member of the Kinesin-1 family. The *khc* loss-of-function mutation is recessive, and early lethal while heterozygous animals do not exhibit any phenotype (Hurd and Saxton, 1996), confirming that the loss of one copy of kinesin-1 is not detrimental. Furthermore, our results were obtained by overexpressing KIF5A  $\Delta$ 27 in *Drosophila* carrying two WT

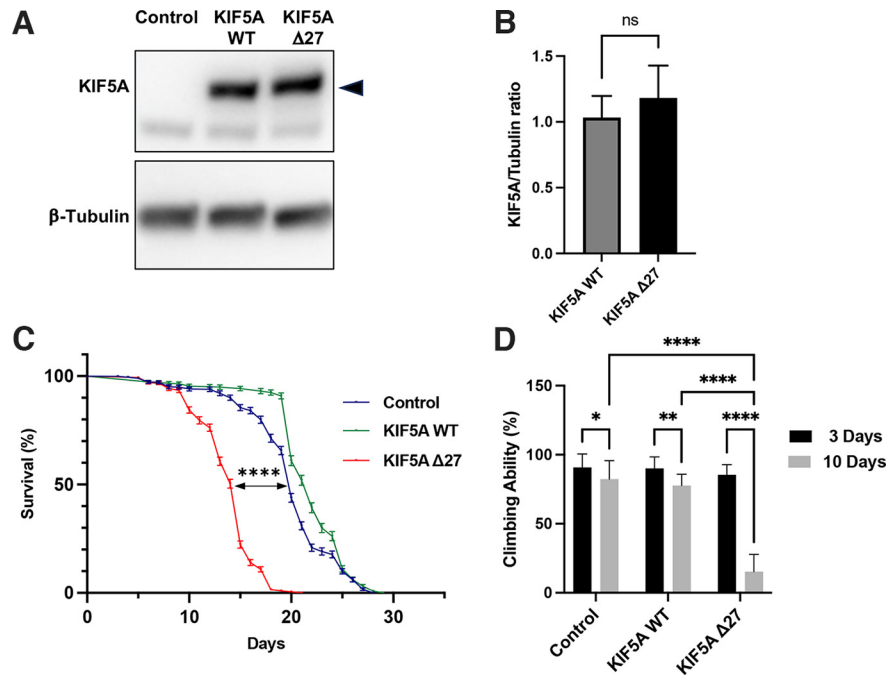


**Figure 9.** In adult motor neurons, expression of KIF5A  $\Delta$ 27 shortens lifespan and reduces climbing activity. **A**, Total protein extraction was performed from the thorax of control (VGlut-Gal4/+), KIF5A WT (VGlut-Gal4/UAS-KIF5A WT), and KIF5A  $\Delta$ 27 (VGlut-Gal4/UAS-KIF5A  $\Delta$ 27) expressing flies. Top, Anti-KIF5A staining (indicated by black arrowhead). Bottom, Anti- $\beta$ -tubulin, used as a loading control. **B**, Quantification of gel bands was done by using Fiji software (Analyze gels); four gels were analyzed. Data are mean  $\pm$  SD. ns,  $p > 0.5$  (Mann-Whitney test). Males shifted at 29°C at eclosion from the VGlut-Gal4, tub-Gal80<sup>15</sup>, UAS KIF5A WT, or KIF5A  $\Delta$ 27 crosses were assayed for lifespan and locomotion assays. **C**, Survival curves at 29°C of male flies VGlut-Gal4; tubGal80<sup>15</sup> control (blue) or expressing KIF5A WT (green) or KIF5A  $\Delta$ 27 (red). The median lifespan is 20 d for control flies, 22 d for KIF5A WT, and 15 d for KIF5A  $\Delta$ 27. Number of flies  $n = 600$ , 450, and 608 for the control, KIF5A WT, and KIF5A  $\Delta$ 27, respectively. Data represent nine different cohorts. Error bars indicate SE. \*\*\*\* $p < 0.0001$  (log-rank test). **D**, Locomotion was monitored by negative geotaxis assays at 3 and 10 d. Three days after the temperature was shifted/raised to 29°C, no difference was observed in the climbing ability of the different genotypes. After 10 d rearing at 29°C, although climbing ability decreased in control and KIF5A WT conditions compared to 3 d as expected, a major effect was observed in the KIF5A  $\Delta$ 27 condition. Compared with the control or KIF5A WT, males expressing KIF5A  $\Delta$ 27 in motor neurons showed an 80% reduction in climbing ability. Number of males considered:  $n = 120$  and 150 for the control at 3 and 10 d, respectively.  $n = 90$  and 150 for KIF5A WT at 3 and 10 d, respectively;  $n = 110$  and 150 for KIF5A  $\Delta$ 27 at 3 and 10 d, respectively. Means  $\pm$  SD are expressed in percentages. \* $p < 0.05$ ; \*\* $p < 0.01$ ; \*\*\*\* $p < 0.0001$ ; two-way ANOVA test with Tukey's multiple comparisons test.

copies of *khc*. The absence of phenotype in *khc*<sup>+/-</sup> heterozygous flies as well as the phenotypes observed after KIF5A  $\Delta$ 27 overexpression argue against a haploinsufficiency effect of KIF5A  $\Delta$ 27 mutations in ALS patients, but rather tend to be explained by a gain-of-function mechanism.

Our results show that one acquired property of KIF5A  $\Delta$ 27 is the ability to form cytoplasmic inclusions, confirming what was described by other studies (Nakano et al., 2022; Pant et al., 2022). Indeed, we observed numerous KIF5A  $\Delta$ 27-positive cytoplasmic inclusions in the soma as well as in the axons of motor neurons. Interestingly, KIF5A  $\Delta$ 27-positive inclusions contain cytoplasmic GFP as well as HRP-positive inclusions. This observation strongly suggests that KIF5A  $\Delta$ 27 is able to recruit neighboring proteins in inclusions, likely explaining the motor neuronal dysfunctions.

Aggregation of KIF5A  $\Delta$ 27 is associated with axonal transport defects, as the distribution of mitochondria as well as synaptic vesicles is strongly altered by KIF5A  $\Delta$ 27 expression. Furthermore, the axonal integrity is also affected, and motor neuron death occurs on KIF5A  $\Delta$ 27 expression. These results are in agreement with those recently reported as KIF5A  $\Delta$ 27 expression induces the death of mouse primary cortical neurons *in vitro* (Baron et al., 2022; Pant et al., 2022) as well as mechanosensory neurons in *Caenorhabditis elegans* (Nakano et al., 2022).

While the pathophysiological mechanisms of ALS are complex, a common signature of the disease is the presence of protein aggregates (Blokhuis et al., 2013). Indeed, many genes associated with familial ALS were prone to aggregation, such as

TDP43 (Neumann et al., 2006), FUS (Kwiatkowski et al., 2009; Vance et al., 2009), SOD1 (Bruijn et al., 1998), and some dipeptide repeat polypeptides originating from C9orf72 hexanucleotide repeat expansion (Al-Sarraj et al., 2011). Our results propose adding KIF5A to the list of aggregation-prone proteins associated with ALS. This is supported by recent studies showing that KIF5A, but not KIF5B or KIF5C, has an intrinsic tendency to oligomerize (Chiba et al., 2022; Pant et al., 2022). Indeed, kinesin-1 generally acts as a homodimer, but it was shown that KIF5A may be found as a tetramer of heavy chains *in vitro* (Chiba et al., 2022).

#### Mitochondria localization is disturbed in KIF5A $\Delta$ 27 condition

The best-known cargos of the kinesin-1 family are mitochondria which play a central role in the life of all cells, but even more in neuronal cells that have high metabolic demands. Indeed, mitochondria play a central role in many metabolism pathways, such as ATP synthesis, calcium homeostasis, or the biogenesis of phospholipids. ATP production and calcium buffering are essential for neuronal life to ensure neurotransmission (Nicholls and Budd, 2000; Rizzuto et al., 2012; Engl and Attwell, 2015). As previous *in vitro* studies have described that the KIF5A  $\Delta$ 27 protein lacks its autoinhibitory property (Baron et al., 2022; Nakano et al., 2022; Pant et al., 2022), we could expect to observe an accumulation of mitochondria at the axonal endings. However, we observed the opposite (i.e., a significant decrease of mitochondria at the NMJs). We believe that, in our comprehensive model, with

sustained metabolic demand, complex biosynthetic activities, and non-cell-autonomous regulatory mechanisms, kinesin-dependent axonal transport can be differentially affected by ALS-causing mutation.

The lack of mitochondria at the NMJs explains why NMJs in KIF5A  $\Delta$ 27-expressing larvae cannot sustain high-frequency stimulation (Guo et al., 2005; Verstreken et al., 2005). Surprisingly, the expression of KIF5A WT induces the same phenotype at the NMJs (i.e., a lack of mitochondria and failure to respond to high frequency stimulation). However, basal neurotransmission remains normal on KIF5A WT expression. In contrast, drastic alterations of neurotransmission were observed on KIF5A  $\Delta$ 27 expression. We propose that the severe reduction in mitochondrial density as well as the presence of mitochondrial inclusions along segmental nerves disturbs the energy supply, leading to neurotransmission defects. This defect in mitochondrial distribution with cluster formation is common to several ALS mouse models (SOD1 G37R or G85R, TDP-43 Q331K or M337V) and is also observed in patients, suggesting that mitochondrial mislocalization is a common pathologic feature in ALS (De Vos et al., 2007; Sasaki and Iwata, 2007; Shan et al., 2010; Velde et al., 2011; Wang et al., 2013; Magrané et al., 2014; Smith et al., 2019).

Beyond mitochondria, we also found that synaptic vesicles are not correctly localized within the axons and at NMJs of KIF5A  $\Delta$ 27-expressing larvae. This suggests a global axonal transport defect induced by KIF5A  $\Delta$ 27. Alteration of motor neuron physiology is supported by aberrant HRP staining, which labels neuronal membranes. In KIF5A  $\Delta$ 27-expressing larvae, HRP staining is not uniform as in control and numerous HRP-positive inclusions were observed, strongly suggesting that the integrity of motor neuron axons is altered. Together, these observations show that, in addition to the defect in mitochondrial localization, the expression of KIF5A  $\Delta$ 27 disrupts the physiological integrity of motor neurons which ultimately leads to their death.

### Cytoskeleton is a central player in ALS

Various mechanisms can explain the onset of ALS, from defects in RNA metabolism, neuronal excitability to altered proteostasis, and intracellular transport. Defects in intracellular trafficking are a general feature found in ALS patients (for review, see Ikenaka et al., 2012; De Vos and Hafezparast, 2017; Burk and Pasterkamp, 2019; Guo et al., 2020). Motor neurons are the largest polarized cells in the human body and axonal transport ensures their homeostasis by allowing both the distribution of lipids and organelles, the transmission of the neuronal signal, and the clearing of misfolded proteins or pathogenic aggregates (Julien and Beaulieu, 2000; Chevalier-Larsen and Holzbaur, 2006; Millicamps and Julien, 2013; Castellanos-Montiel et al., 2020; Theunissen et al., 2021). This process is only possible if the integrity of the neuronal cytoskeleton is maintained, giving the cytoskeleton a central role in neuronal cells.

To date, ~30 ALS-related genes have been identified, with four of them directly involved in microtubule dynamics. The *TUBA4A* gene encoding tubulin  $\alpha$  4a protein and the Spastin protein (an ATPase) are involved in the formation and disassembly of microtubule tracks, respectively. The other two genes, *DCTN1* (Dynactin subunit 1) and *KIF5A*, are microtubule-related molecular motors implied in retrograde (via Dynein binding) and anterograde transport, respectively. However, these genes only account for <5% of all ALS cases (Liu and Henty-Ridilla, 2022). This low representation does not match with the axonal transport defects observed in patients. Interestingly, SOD1, FUS, TDP43, and

C9orf72 variants, which are responsible for the majority of familial ALS cases, are also known to directly or indirectly cause axonal transport and/or mitochondrial defects (Burk and Pasterkamp, 2019; W. Guo et al., 2020). This observation reinforces the hypothesis that cytoskeleton dynamics (and, more specifically, microtubule disorganization) can trigger axonal degeneration and synapse loss, raising the question of oligogenic etiology in ALS.

Here, we characterize the alterations induced by the expression of the ALS-associated KIF5A mutant in *Drosophila* motor neurons. In this whole organism, expression of KIF5A  $\Delta$ 27 selectively in motor neurons leads to behavioral locomotor deficits associated with morphologic alteration of the NMJs. Moreover, the observed tail-flipping phenotype suggests an impairment of axonal transport that is reinforced by a failure of neurotransmission recorded at the synaptic level. In addition, KIF5A  $\Delta$ 27 containing cytoplasmic inclusions are found in the soma and axons of motor neurons. Finally, the expression of KIF5A  $\Delta$ 27 leads to motor neuronal loss and *Drosophila* death when its expression is reinforced. This *in vivo* study shows that the pathogenicity of KIF5A mutant to motor neurons arises from a toxic gain of function and represents an important step in our understanding of the pathogenesis of ALS.

### References

- Al-Sarraj S, King A, Troakes C, Smith B, Maekawa S, Bodi I, Rogelj B, Al-Chalabi A, Hortobágyi T, Shaw CE (2011) p62 positive, TDP-43 negative, neuronal cytoplasmic and intranuclear inclusions in the cerebellum and hippocampus define the pathology of C9orf72-linked FTL and MND/ALS. *Acta Neuropathol* 122:691–702.
- Baron DM, et al. (2022) ALS-associated KIF5A mutations abolish autoinhibition resulting in a toxic gain of function. *Cell Rep* 39:110598.
- Bilen J, Bonini NM (2005) *Drosophila* as a model for human neurodegenerative disease. *Annu Rev Genet* 39:153–171.
- Blair MA, Ma S, Hedera P (2006) Mutation in KIF5A can also cause adult-onset hereditary spastic paraplegia. *Neurogenetics* 7:47–50.
- Blokhuis AM, Groen EJ, Koppers M, van den Berg LH, Pasterkamp RJ (2013) Protein aggregation in amyotrophic lateral sclerosis. *Acta Neuropathol* 125:777–794.
- Brady ST (1985) A novel brain ATPase with properties expected for the fast axonal transport motor. *Nature* 317:73–75.
- Brand AH, Manoukian AS, Perrimon N (1994) Ectopic expression in *Drosophila*. *Methods Cell Biol* 44:635–654.
- Brand AH, Perrimon N (1993) Targeted gene expression as a means of altering cell fates and generating dominant phenotypes. *Development* 118:401–415.
- Brenner D, et al., German ALS network MND-NET (2018) Hot-spot KIF5A mutations cause familial ALS. *Brain* 141:688–697.
- Brujin LI, Houseweart MK, Kato S, Anderson KL, Anderson SD, Ohama E, Reaume AG, Scott RW, Cleveland DW (1998) Aggregation and motor neuron toxicity of an ALS-linked SOD1 mutant independent from wild-type SOD1. *Science* 281:1851–1854.
- Budnik V, Koh YH, Guan B, Hartmann B, Hough C, Woods D, Gorczyca M (1996) Regulation of synapse structure and function by the *Drosophila* tumor suppressor gene *dlg*. *Neuron* 17:627–640.
- Burk K, Pasterkamp RJ (2019) Disrupted neuronal trafficking in amyotrophic lateral sclerosis. *Acta Neuropathol* 137:859–877.
- Campbell PD, Shen K, Sapio MR, Glenn TD, Talbot WS, Marlow FL (2014) Unique function of kinesin Kif5A in localization of mitochondria in axons. *J Neurosci* 34:14717–14732.
- Cason SE, Holzbaur EL (2022) Selective motor activation in organelle transport along axons. *Nat Rev Mol Cell Biol* 23:699–714.
- Castellanos-Montiel MJ, Chaineau M, Durcan TM (2020) The neglected genes of ALS: cytoskeletal dynamics impact synaptic degeneration in ALS. *Front Cell Neurosci* 14:594975.
- Chevalier-Larsen E, Holzbaur EL (2006) Axonal transport and neurodegenerative disease. *Biochim Biophys Acta* 1762:1094–1108.

- Chiba K, Ori-McKenney KM, Niwa S, McKenney RJ (2022) Synergistic auto-inhibition and activation mechanisms control kinesin-1 motor activity. *Cell Rep* 39:110900.
- Cleveland DW, Rothstein JD (2001) From Charcot to Lou Gehrig: deciphering selective motor neuron death in ALS. *Nat Rev Neurosci* 2:806–819.
- Crimella C, Baschiroto C, Arnoldi A, Tonelli A, Tenderini E, Airolidi G, Martinuzzi A, Trabacca A, Losito L, Scarlato M, Benedetti S, Scarpini E, Spinicci G, Bresolin N, Bassi MT (2012) Mutations in the motor and stalk domains of KIF5A in spastic paraplegia type 10 and in axonal Charcot-Marie-Tooth type 2. *Clin Genet* 82:157–164.
- de Fuenmayor-Fernández de la Hoz CP, Hernández-Lain A, Olivé M, Sánchez-Calvín MT, Gonzalo-Martínez JF, Domínguez-González C (2019) Adult-onset distal spinal muscular atrophy: a new phenotype associated with KIF5A mutations. *Brain* 142:e66.
- De Vos KJ, Hafezparast M (2017) Neurobiology of axonal transport defects in motor neuron diseases: opportunities for translational research? *Neurobiol Dis* 105:283–299.
- De Vos KJ, Chapman AL, Tennant ME, Manser C, Tudor EL, Lau KF, Brownlees J, Ackerley S, Shaw PJ, McLoughlin DM, Shaw CE, Leigh PN, Miller CC, Grierson AJ (2007) Familial amyotrophic lateral sclerosis-linked SOD1 mutants perturb fast axonal transport to reduce axonal mitochondria content. *Hum Mol Genet* 16:2720–2728.
- Devambaz I, van Dijk J, Benlefski S, Layalle S, Grau Y, Rogowski K, Parmentier ML, Soustelle L (2017) Identification of DmTTL5 as a major tubulin glutamylase in the *Drosophila* nervous system. *Sci Rep* 7:16254.
- Duis J, Dean S, Applegate C, Harper A, Xiao R, He W, Dollar JD, Sun LR, Waberski MB, Crawford TO, Hamosh A, Stafstrom CE (2016) KIF5A mutations cause an infantile onset phenotype including severe myoclonus with evidence of mitochondrial dysfunction. *Ann Neurol* 80:633–637.
- Engl E, Attwell D (2015) Non-signalling energy use in the brain. *J Physiol* 593:3417–3429.
- Fichera M, Lo Giudice M, Falco M, Sturnio M, Amata S, Calabrese O, Bigoni S, Calzolari E, Neri M (2004) Evidence of kinesin heavy chain (KIF5A) involvement in pure hereditary spastic paraplegia. *Neurology* 63:1108–1110.
- Freeman M (1996) Reiterative use of the EGF receptor triggers differentiation of all cell types in the *Drosophila* eye. *Cell* 87:651–660.
- Füger P, Sreekumar V, Schüle R, Kern JV, Stanchew DT, Schneider CD, Karle KN, Daub KJ, Siegert VK, Flötenmeyer M, Schwarz H, Schöls L, Rasse TM (2012) Spastic paraplegia mutation N256S in the neuronal microtubule motor KIF5A disrupts axonal transport in a *Drosophila* HSP model. *PLoS Genet* 8:e1003066.
- Gerasimavicius L, Livesey BJ, Marsh JA (2022) Loss-of-function, gain-of-function and dominant-negative mutations have profoundly different effects on protein structure. *Nat Commun* 13:3895.
- Gregory JM, Fagegaltier D, Phatnani H, Harms MB (2020) Genetics of amyotrophic lateral sclerosis. *Curr Genet Med Rep* 8:121–131.
- Guillaud L, El-Agamy SE, Otsuki M, Terenzio M (2020) Anterograde axonal transport in neuronal homeostasis and disease. *Front Mol Neurosci* 13:556175.
- Guo W, Fumagalli L, Van Den Bosch L (2020) Targeting axonal transport: a new therapeutic avenue for ALS. In: *Amyotrophic lateral sclerosis: recent advances and therapeutic challenges* (Hegde M, ed). IntechOpen. <https://www.intechopen.com/books/amyotrophic-lateral-sclerosis-recent-advances-and-therapeutic-challenges/targeting-axonal-transport-a-new-therapeutic-avenue-for-als>.
- Guo X, Macleod GT, Wellington A, Hu F, Panchumarthi S, Schoenfield M, Marin L, Charlton MP, Atwood HL, Zinsmaier KE (2005) The GTPase dMiro is required for axonal transport of mitochondria to *Drosophila* synapses. *Neuron* 47:379–393.
- Hirokawa N, Takemura R (2005) Molecular motors and mechanisms of directional transport in neurons. *Nat Rev Neurosci* 6:201–214.
- Hirokawa N, Pfister KK, Yorifuji H, Wagner MC, Brady ST, Bloom GS (1989) Submolecular domains of bovine brain kinesin identified by electron microscopy and monoclonal antibody decoration. *Cell* 56:867–878.
- Hunter B, Allingham JS (2020) These motors were made for walking. *Protein Sci* 29:1707–1723.
- Hurd DD, Saxton WM (1996) Kinesin mutations cause motor neuron disease phenotypes by disrupting fast axonal transport in *Drosophila*. *Genetics* 144:1075–1085.
- Ikenaka K, Katsuno M, Kawai K, Ishigaki S, Tanaka F, Sobue G (2012) Disruption of axonal transport in motor neuron diseases. *Int J Mol Sci* 13:1225–1238.
- Imlach W, McCabe BD (2009) Electrophysiological methods for recording synaptic potentials from the NMJ of *Drosophila* larvae. *J Vis Exp* 24:1109.
- Julien JP, Beaulieu JM (2000) Cytoskeletal abnormalities in amyotrophic lateral sclerosis: beneficial or detrimental effects? *J Neurol Sci* 180:7–14.
- Kanai Y, Okada Y, Tanaka Y, Harada A, Terada S, Hirokawa N (2000) KIF5C, a novel neuronal kinesin enriched in motor neurons. *J Neurosci* 20:6374–6384.
- Karle KN, Möckel D, Reid E, Schöls L (2012) Axonal transport deficit in a KIF5A (–/–) mouse model. *Neurogenetics* 13:169–179.
- Kauwe G, Isacoff EY (2013) Rapid feedback regulation of synaptic efficacy during high-frequency activity at the *Drosophila* larval neuromuscular junction. *Proc Natl Acad Sci USA* 110:9142–9147.
- Kawaguchi K (2013) Role of kinesin-1 in the pathogenesis of SPG10, a rare form of hereditary spastic paraplegia. *Neuroscientist* 19:336–344.
- Kwiatkowski TJ, et al. (2009) Mutations in the FUS/TLS gene on chromosome 16 cause familial amyotrophic lateral sclerosis. *Science* 323:1205–1208.
- Landgraf M, Jeffrey V, Fujioka M, Jaynes JB, Bate M (2003) Embryonic origins of a motor system: motor dendrites form a myotopic map in *Drosophila*. *PLoS Biol* 1:E41.
- Lelieveld SH, Wiel L, Venselaar H, Pfundt R, Vriend G, Veltman JA, Brunner HG, Vissers LE, Gilissen C (2017) Spatial clustering of de novo missense mutations identifies candidate neurodevelopmental disorder-associated genes. *Am J Hum Genet* 101:478–484.
- Liu X, Henty-Ridilla JL (2022) Multiple roles for the cytoskeleton in ALS. *Exp Neurol* 355:114143.
- Livesey BJ, Marsh JA (2022) The properties of human disease mutations at protein interfaces. *PLoS Comput Biol* 18:e1009858.
- Magrané J, Cortez C, Gan WB, Manfredi G (2014) Abnormal mitochondrial transport and morphology are common pathological denominators in SOD1 and TDP43 ALS mouse models. *Hum Mol Genet* 23:1413–1424.
- Mahr A, Aberle H (2006) The expression pattern of the *Drosophila* vesicular glutamate transporter: a marker protein for motoneurons and glutamatergic centers in the brain. *Gene Expr Patterns* 6:299–309.
- Martin M, Iyadurai SJ, Gassman A, Gindhart JG, Hays TS, Saxton WM (1999) Cytoplasmic dynein, the dynactin complex, and kinesin are interdependent and essential for fast axonal transport. *Mol Biol Cell* 10:3717–3728.
- Martinez VG, Javadi CS, Ngo E, Ngo L, Lagow RD, Zhang B (2007) Age-related changes in climbing behavior and neural circuit physiology in *Drosophila*. *Dev Neurobiol* 67:778–791.
- Menon KP, Carrillo RA, Zinn K (2013) Development and plasticity of the *Drosophila* larval neuromuscular junction. *Wiley Interdiscip Rev Dev Biol* 2:647–670.
- Miki H, Setou M, Kaneshiro K, Hirokawa N (2001) All kinesin superfamily protein, KIF, genes in mouse and human. *Proc Natl Acad Sci USA* 98:7004–7011.
- Millecamps S, Julien JP (2013) Axonal transport deficits and neurodegenerative diseases. *Nat Rev Neurosci* 14:161–176.
- Mudher A, Shepherd D, Newman TA, Mildren P, Jukes JP, Squire A, Mears A, Drummond JA, Berg S, MacKay D, Asuni AA, Bhat R, Lovestone S (2004) GSK-3 $\beta$  inhibition reverses axonal transport defects and behavioural phenotypes in *Drosophila*. *Mol Psychiatry* 9:522–530.
- Nakajima K, Yin X, Takei Y, Seog DH, Homma N, Hirokawa N (2012) Molecular motor KIF5A is essential for GABAA receptor transport, and KIF5A deletion causes epilepsy. *Neuron* 76:945–961.
- Nakano J, Chiba K, Niwa S (2022) An ALS-associated KIF5A mutant forms oligomers and aggregates and induces neuronal toxicity. *Genes Cells* 27:421–435.
- Nam DE, Yoo DH, Choi SS, Choi BO, Chung KW (2018) Wide phenotypic spectrum in axonal Charcot-Marie-Tooth neuropathy type 2 patients with KIF5A mutations. *Genes Genomics* 40:77–84.
- Neumann M, Sampathu DM, Kwong LK, Truax AC, Micsenyi MC, Chou TT, Bruce J, Schuck T, Grossman M, Clark CM, McCluskey LF, Miller BL, Masliah E, Mackenzie IR, Feldman H, Feiden W, Kretschmar HA, Trojanowski JQ, Lee VM (2006) Ubiquitinated TDP-43 in frontotemporal lobar degeneration and amyotrophic lateral sclerosis. *Science* 314:130–133.

- Newman ZL, Hoagland A, Aghi K, Worden KL, Levy SL, Son JH, Lee LP, Isacoff EY (2017) Input-specific plasticity and homeostasis at the *Drosophila* larval neuromuscular junction. *Neuron* 93:1388–1404.e10.
- Nicholls DG, Budd SL (2000) Mitochondria and neuronal survival. *Physiol Rev* 80:315–360.
- Nicolas A, et al., Project MinE ALS Sequencing Consortium (2018) Genome-wide analyses identify KIF5A as a novel ALS gene. *Neuron* 97:1268–1283.e6.
- Pant DC, Parameswaran J, Rao L, Loss I, Chilukuri G, Parlato R, Shi L, Glass JD, Bassell GJ, Koch P, Yilmaz R, Weishaupt JH, Gennerich A, Jiang J (2022) ALS-linked KIF5A  $\Delta$ Exon27 mutant causes neuronal toxicity through gain-of-function. *EMBO Rep* 23:e54234.
- Park JH, Schroeder AJ, Helfrich-Förster C, Jackson FR, Ewer J (2003) Targeted ablation of CCAP neuropeptide-containing neurons of *Drosophila* causes specific defects in execution and circadian timing of ecdysis behavior. *Development* 130:2645–2656.
- Pilling AD, Horiuchi D, Lively CM, Saxton WM (2006) Kinesin-1 and Dynein are the primary motors for fast transport of mitochondria in *Drosophila* motor axons. *Mol Biol Cell* 17:2057–2068.
- Qin J, Zhang H, Geng Y, Ji Q (2020) How kinesin-1 utilize the energy of nucleotide: the conformational changes and mechanochemical coupling in the unidirectional motion of kinesin-1. *Int J Mol Sci* 21:E6977.
- Qiu Y, Zhong S, Cong L, Xin L, Gao X, Zhang J, Hong D (2018) A novel KIF5A gene variant causes spastic paraplegia and cerebellar ataxia. *Ann Clin Transl Neurol* 5:1415–1420.
- Reid E, Kloos M, Ashley-Koch A, Hughes L, Bevan S, Svenson IK, Graham FL, Gaskell PC, Dearlove A, Pericak-Vance MA, Rubinsztein DC, Marchuk DA (2002) A kinesin heavy chain (KIF5A) mutation in hereditary spastic paraplegia (SPG10). *Am J Hum Genet* 71:1189–1194.
- Rizzuto R, De Stefani D, Raffaello A, Mammucari C (2012) Mitochondria as sensors and regulators of calcium signalling. *Nat Rev Mol Cell Biol* 13:566–578.
- Rydzanicz M, Jagła M, Kosinska J, Tomasik T, Sobczak A, Pollak A, Herman-Sucharska I, Walczak A, Kwinta P, Płoski R (2017) KIF5A de novo mutation associated with myoclonic seizures and neonatal onset progressive leukoencephalopathy. *Clin Genet* 91:769–773.
- Sasaki S, Iwata M (2007) Mitochondrial alterations in the spinal cord of patients with sporadic amyotrophic lateral sclerosis. *J Neuropathol Exp Neurol* 66:10–16.
- Shan X, Chiang PM, Price DL, Wong PC (2010) Altered distributions of Gemini of coiled bodies and mitochondria in motor neurons of TDP-43 transgenic mice. *Proc Natl Acad Sci USA* 107:16325–16330.
- Smith EF, Shaw PJ, De Vos KJ (2019) The role of mitochondria in amyotrophic lateral sclerosis. *Neurosci Lett* 710:132933.
- Theunissen F, West PK, Brennan S, Petrović B, Hooshmand K, Akkari PA, Keon M, Guennevig B (2021) New perspectives on cytoskeletal dysregulation and mitochondrial mislocalization in amyotrophic lateral sclerosis. *Transl Neurodegener* 10:46.
- Valle RD, Reese TS, Sheetz MP (1985) Identification of a novel force-generating protein, kinesin, involved in microtubule-based motility. *Cell* 42:39–50.
- Vance C, et al. (2009) Mutations in FUS, an RNA processing protein, cause familial amyotrophic lateral sclerosis type 6. *Science* 323:1208–1211.
- Velde CV, McDonald KK, Boukhedimi Y, McAlonis-Downes M, Lobsiger CS, Hadj SB, Zandona A, Julien JP, Shah SB, Cleveland DW (2011) Misfolded SOD1 associated with motor neuron mitochondria alters mitochondrial shape and distribution prior to clinical onset. *PLoS One* 6:e22031.
- Verstreken P, Ly CV, Venken KJ, Koh TW, Zhou Y, Bellen HJ (2005) Synaptic mitochondria are critical for mobilization of reserve pool vesicles at *Drosophila* neuromuscular junctions. *Neuron* 47:365–378.
- Wagh DA, Rasse TM, Asan E, Hofbauer A, Schwenkert I, Dürrbeck H, Buchner S, Dabauvalle MC, Schmidt M, Qin G, Wichmann C, Kittel R, Sigrist SJ, Buchner E (2006) Bruchpilot, a protein with homology to ELKS/CAST, is required for structural integrity and function of synaptic active zones in *Drosophila*. *Neuron* 49:833–844.
- Wang L, Brown A (2010) A hereditary spastic paraplegia mutation in kinesin-1A/KIF5A disrupts neurofilament transport. *Mol Neurodegener* 5:52.
- Wang W, Li L, Lin WL, Dickson DW, Petrucelli L, Zhang T, Wang X (2013) The ALS disease-associated mutant TDP-43 impairs mitochondrial dynamics and function in motor neurons. *Hum Mol Genet* 22:4706–4719.
- Xia CH, Roberts EA, Her LS, Liu X, Williams DS, Cleveland DW, Goldstein LS (2003) Abnormal neurofilament transport caused by targeted disruption of neuronal kinesin heavy chain KIF5A. *J Cell Biol* 161:55–66.